A novel comparison framework for epidemiological strategies applied to age-based restrictions versus horizontal lockdowns

Vasiliki Bitsouni [a, *, 1], Nikolaos Gialelis [b, c, 2], Vasilis Tsilidis [a, 3]

[a] *Department of Mathematics, University of Patras, GR-26504, Rio Patras, Greece*
[b] *Department of Mathematics, National and Kapodistrian University of Athens, GR-15784, Athens, Greece*
[c] *School of Medicine, National and Kapodistrian University of Athens, GR-11527, Athens, Greece*

ARTICLE INFO

ABSTRACT

During an epidemic, such as the COVID-19 pandemic, policy-makers are faced with the decision of implementing effective, yet socioeconomically costly intervention strategies, such as school and workplace closure, physical distancing, etc. In this study, we propose a rigorous definition of epidemiological strategies. In addition, we develop a scheme for comparing certain epidemiological strategies, with the goal of providing policy-makers with a tool for their systematic comparison. Then, we put the suggested scheme to the test by employing an age-based epidemiological compartment model introduced in Bitsouni et al. (2024), coupled with data from the literature, in order to compare the effectiveness of age-based and horizontal interventions. In general, our findings suggest that these two are comparable, mainly at a low or medium level of intensity.

© 2024 The Authors. Publishing services by Elsevier B.V. on behalf of KeAi Communications Co. Ltd. This is an open access article under the CC BY-NC-ND license (http://creativecommons.org/licenses/by-nc-nd/4.0/).

1. Introduction

The recent COVID-19 pandemic brought to the fore the disastrous for the economy consequences of horizontal lockdowns. Economically costly horizontal measures during the COVID-19 pandemic have been the closure of workplaces and schools, the cancellation of public events and general stay-at-home restrictions (see Brodeur et al. (2021), Chen et al. (2021), Deb et al. (2021), Mathieu et al. (2020) and many references therein).

This fact highlights the need for a more sophisticated managing of epidemiological crises. In this context, many countries, especially after the spasmodic first response, have looked for more flexible intervention policies. Multiple combinations of interventions were deployed by policy-makers in order to combat the spread of SARS-CoV-2 and minimize their impact on the economy (Asahi et al., 2021; Karatayev et al., 2020; Perra, 2021).

Finding ways to intervene in the natural progression of disease spreading, has been a hot topic in the scientific community. Models have been proposed, for a wide range of diseases, investigating various non-pharmaceutical interventions (Adegbite et al., 2023; Amaku et al., 2021; Bhadauria et al., 2023; Brethouwer et al., 2021; Demers et al., 2023; Saha et al., 2022; Vatcheva et al., 2021; Verma et al., 2020; Zakary et al., 2017), vaccination (Abell et al., 2023; Anupong et al., 2023; Gan et al., 2024; Owusu-Dampare & Bouchnita, 2023; Patón et al., 2023; Thongtha & Modnak, 2022) and treatment (Béraud et al., 2022; Zaman et al., 2009) strategies, as well as various combinations of the aforementioned interventions (Apenteng et al., 2020; Lamba et al., 2024). Despite the success of the foregoing studies, the lack of a mathematically rigorous definition of epidemiological strategies is apparent.

Moreover, age-based interventions have been discussed as a theoretical alternative to horizontal lockdowns. However, they have also raised ethical concerns with regard to ageism (Motorniak et al., 2023; Spaccatini et al., 2022; Van Rens & Oswald, 2020).

To our knowledge, the investigation of age-based interventions has been limited in terms of modeling. The authors of Acemoglu et al. (2021) proposed a multigroup SIR model, with the intent of studying age-based lockdowns. In Kirwin et al. (2021), the authors study the prioritization of vaccination to selected target groups.

In the present study, we:

— give a rigorous definition of the notion of epidemiological strategies
— propose a framework for systematically comparing certain epidemiological strategies
— utilize the aforementioned scheme to compare the effectiveness of age-based interventions when compared to horizontal lockdowns, in the case of the SARS-CoV-2 pandemic.

This study is organized as follows. In §2, we introduce the notion of an (epidemiological) strategy, along with its potential gradations, and we present a framework for comparing the effectiveness of certain strategies. In §3, we contrast the impact of a horizontal lockdown with varying levels of intensity, with certain age-based countermeasures that have a similar epidemiological effect, but less of an influence on society and, consequently, the economy. In §4, we conclude with a summary and discussion of the results.

2. A framework for comparing the effectiveness of different strategies

Let us divide a population into two classes, the infectious, $\mathcal{I}$, and the non-infectious, $\mathcal{I}^c$. Each of these classes can be divided to further sub-compartments, e.g., $A \in \mathcal{I}$ and $B \in \mathcal{I}^c$.

The *transmission rate* from compartment B to compartment A is defined as

$$\beta_{B \to A} := \frac{c_B \cdot \varpi_{B \to A}}{N}, \tag{1}$$

where c_B is the average number of close contacts of an individual belonging in B with other individuals, $\varpi_{B \to A}$ is the probability of a contact to be effective in turning an individual of compartment B to an individual of compartment A, and

$$N := \mathcal{I} + \mathcal{I}^c$$

is the total number of the population. The *removal rate* from compartment A to compartment B is defined as

$$\gamma_{A \to B} := \frac{1}{P_{A \to B}}, \tag{2}$$

where $P_{A \to B}$ is the average period an individual spends on compartment A before moving into compartment B. A diagram for the above definitions is shown in Fig. 1.

These parameters, probably among others depending on the model (for instance, the model employed later on in the present study comprises two types of transmission rates and two types of removal rates, among nine other parameters), are
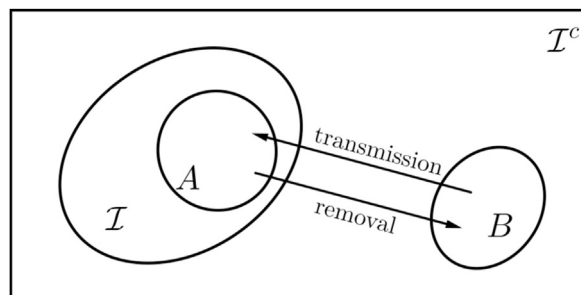

Fig. 1. Flows between the classes of infectious, $\mathcal{I}$, and non-infectious, $\mathcal{I}^c$, individuals of a population.

involved into the formulation of an epidemiological model that describes an epidemiological problem under study. However, these parameters are special, because interventions by external factors acting for the control of the studied epidemiological phenomenon (e.g., policy makers), can be described as changes in their values.

Now, enumerating all the different transmission and removal rates of a particular model, i.e., $\beta_1, ..., \beta_{n_1}$ and $\gamma_1, ..., \gamma_{n_2}$, respectively, we can write

$$\boldsymbol{\beta} = (\beta_i)_{i=1}^{n_1} \text{ and } \boldsymbol{\gamma} = (\gamma_i)_{i=1}^{n_2}.$$

Throughout the present section we assume a well-posed global (with respect to time) epidemiological compartmental problem,

$$\mathscr{P} = \mathscr{P}(\mathscr{M}),$$

which is described by a (differential/difference equations, agent-based, etc.) model,

$$\mathscr{M} = \mathscr{M}(\boldsymbol{x}, (\boldsymbol{\beta}(\boldsymbol{x}), \boldsymbol{\gamma}(\boldsymbol{x})), \boldsymbol{\delta}(\boldsymbol{x})),$$

where

$$\boldsymbol{x} = (x_i)_{i=1}^m \in \mathcal{X} \subseteq \mathbb{R}^m$$

is the vector of the independent variables,

$$(\boldsymbol{\beta}, \boldsymbol{\gamma}) \in F(\mathcal{X}; \mathcal{P}_{\text{tr,r}} \subseteq \mathbb{R}^{n_1} \times \mathbb{R}^{n_2}) = \{\boldsymbol{f} : \mathcal{X} \to \mathcal{P}_{\text{tr,r}}\}$$

is the vector-valued function of the parameters of interest of $\mathscr{M}$ and

$$\boldsymbol{\delta} \in F(\mathcal{X}; \mathcal{P}_{\text{other}} \subseteq \mathbb{R}^{n_3})$$

is the vector-valued function of the rest of parameters of $\mathscr{M}$.

2.1. Strategies and substrategies

We begin by introducing the concept of a *strategy* of $\mathscr{P}$, which is of pivotal importance for the following analysis. In the epidemiology framework, a strategy can be considered as the mathematical description of a set of epidemiological interventions made by potential external factors, such as policy makers, experts etc., in order to restrict the epidemiological phenomenon. These interventions consist of first fixing a reference value, $(\boldsymbol{\beta}_0, \boldsymbol{\gamma}_0) \in F(\mathcal{X}; \mathcal{P}_{\text{tr,r}})$, for the parameters chosen, and then scaling each element of the set in terms of the fixed value.

Defintion 1. (strategy & strategic scale of an element). *Let $(\boldsymbol{\beta}_0, \boldsymbol{\gamma}_0) \in F(\mathcal{X}; \mathcal{P}_{\text{tr,r}})$.*

1. A set $S = S(\boldsymbol{\beta}_0, \boldsymbol{\gamma}_0) \subseteq F(\mathcal{X}; \mathcal{P}_{\text{tr,r}})$ is called strategy (of $\mathscr{P}$) with respect to $(\boldsymbol{\beta}_0, \boldsymbol{\gamma}_0)$ iff

$$\forall \boldsymbol{y} \in S \ \exists \boldsymbol{r} = \boldsymbol{r}(\cdot; (\boldsymbol{\beta}_0, \boldsymbol{\gamma}_0), \boldsymbol{y}) \in F(\mathcal{X}; \mathbb{R}^{n_1+n_2}) \text{ s.t. } \boldsymbol{y} = \boldsymbol{r} \odot (\boldsymbol{\beta}_0, \boldsymbol{\gamma}_0),$$

where $\odot$ stands for the Hadamard product.

2. Let
  i. $S = S(\boldsymbol{\beta}_0, \boldsymbol{\gamma}_0)$ be a respective strategy and
  ii. $\boldsymbol{y} \in S$.

A function $\boldsymbol{r} \in F(\mathcal{X}; \mathbb{R}^{n_1+n_2})$ as in 1. is called strategic scale of $\boldsymbol{y}$.

We observe that every subset of a strategy is a strategy itself, as it is referred in the following result, the elementary proof of which is omitted.

Proposition 1. *Let*

1. $(\boldsymbol{\beta}_0, \boldsymbol{\gamma}_0) \in F(\mathcal{X}; \mathcal{P}_{\text{tr,r}})$,
2. $S = S(\boldsymbol{\beta}_0, \boldsymbol{\gamma}_0)$ be a respective strategy and
3. $S_0 \subseteq S$.

Then S_0 is a strategy with respect to $(\boldsymbol{\beta}_0, \boldsymbol{\gamma}_0)$.

In view of Proposition 1, we give the definition of a substrategy of a given strategy. In the epidemiology framework, a *substrategy* can be considered as the mathematical description of a subset of a given set of epidemiological interventions.

Defintion 2. (substrategy). *Let*

  i. $(\boldsymbol{\beta}_0, \boldsymbol{\gamma}_0) \in F(\mathcal{X}; \mathcal{P}_{\mathrm{tr,r}})$,
  ii. $S = S(\boldsymbol{\beta}_0, \boldsymbol{\gamma}_0)$ *be a respective strategy and*
  iii. $S_0 \subseteq S$.

We call S_0 a substrategy of S.

In fact, we can define a substrategy by setting limitations to the choice of a strategic scale of each of its elements. Below, we name certain such examples.

Defintion 3. (horizontal and x_i-based strategy). *Let*

  i. $(\boldsymbol{\beta}_0, \boldsymbol{\gamma}_0) \in F(\mathcal{X}; \mathcal{P}_{\mathrm{tr,r}})$,
  ii. $S = S(\boldsymbol{\beta}_0, \boldsymbol{\gamma}_0)$ *be a respective strategy and*
  iii. $S_0 \subseteq S$.

We name the following substrategies.

1. *Let $i \in \{1, \ldots, m\}$. S_0 is called horizontal with respect to x_i iff*

$$\boldsymbol{r}(\boldsymbol{x}; (\boldsymbol{\beta}_0, \boldsymbol{\gamma}_0), \boldsymbol{y}) = \boldsymbol{r}(x_1, \ldots, x_{i-1}, x_{i+1}, \ldots, x_m; (\boldsymbol{\beta}_0, \boldsymbol{\gamma}_0), \boldsymbol{y}), \ \forall \boldsymbol{x} \in \mathcal{X}, \ \forall \boldsymbol{y} \in S_0,$$

i.e., $\forall \boldsymbol{y} \in S_0$ a respective strategic scale is independent of x_i, otherwise we call it x_i-based.

2. *S_0 is called horizontal, iff it is horizontal with respect to x_i, $\forall i \in \{1, \ldots, m\}$.*

In the epidemiology framework, a x_i-based substrategy can be considered as the mathematical description of a subset of epidemiological interventions, which targets a certain group of a population partitioned with respect to x_i variable.

We also observe that every union of strategies is a strategy itself, as it is referred in the following elementary result.

Proposition 2. *Let*

1. $(\boldsymbol{\beta}_0, \boldsymbol{\gamma}_0) \in F(\mathcal{X}; \mathcal{P}_{\mathrm{tr,r}})$ *and*
2. $\{S_j = S_j(\boldsymbol{\beta}_0, \boldsymbol{\gamma}_0)\}_{j \in \mathcal{J}}$ *be a family of respective strategies.*

Then $\bigcup_{j \in \mathcal{J}} S_j$ is a strategy with respect to $(\boldsymbol{\beta}_0, \boldsymbol{\gamma}_0)$.

In view of Proposition 2, we give the following definition.

Defintion 4. (the largest strategy). *Let*

1. $(\boldsymbol{\beta}_0, \boldsymbol{\gamma}_0) \in F(\mathcal{X}; \mathcal{P}_{\mathrm{tr,r}})$ *and*
2. $\mathcal{S}$ *be the family of all the respective strategies.*

We call

$$\hat{S} = \hat{S}(\boldsymbol{\beta}_0, \boldsymbol{\gamma}_0) = \bigcup_{S \in \mathcal{S}} S$$

the largest strategy with respect to $(\boldsymbol{\beta}_0, \boldsymbol{\gamma}_0)$.

Of course, whatever result holds for the largest strategy also holds for an abstract strategy, like the following direct one.

Proposition 3. *Let $(\boldsymbol{\beta}_0, \boldsymbol{\gamma}_0) \in F(\mathcal{X}; \mathcal{P}_{\mathrm{tr,r}})$. If*

$$\left(\underbrace{0, \ldots, 0}_{\# \ n_1 + n_2} \right) \notin (\boldsymbol{\beta}_0(\mathcal{X}), \boldsymbol{\gamma}_0(\mathcal{X})), \tag{3}$$

then

$\forall \boldsymbol{y} \in \hat{S} \ \exists !$ *strategic scale of* $\boldsymbol{y}$.

Under the light of Proposition 3, the next notion is well-defined.

Defintion 5.   (strategic scale of a strategy). *Let*

1. $(\boldsymbol{\beta}_0, \boldsymbol{\gamma}_0) \in F(\mathcal{X}; \mathcal{P}_{tr,r})$ *satisfy* (3) *and*
2. $S = S(\boldsymbol{\beta}_0, \boldsymbol{\gamma}_0)$ *be a respective strategy.*

We call the function

$$S \ni \boldsymbol{y} \mapsto \boldsymbol{r}(\ \cdot\ ; (\boldsymbol{\beta}_0, \boldsymbol{\gamma}_0), \boldsymbol{y}) \in F(\mathcal{X}; \mathbb{R}^{n_1+n_2})$$

the strategic scale of S.

We can then easily deduce the following result.

Proposition 4.   *Let*

  i. $(\boldsymbol{\beta}_0, \boldsymbol{\gamma}_0) \in F(\mathcal{X}; \mathcal{P}_{tr,r})$ *satisfy* (3),
 ii. $S = S(\boldsymbol{\beta}_0, \boldsymbol{\gamma}_0)$ *be a respective strategy,*
iii. $\mathfrak{P}_j$, $\forall j \in \{1, 2\}$ *be mathematical statements with respect to the strategic scale of S such that* $\mathfrak{P}_1 \Rightarrow \mathfrak{P}_2$ *and*
 iv. $S_j \subseteq S$, $\forall j \in \{1, 2, 3\}$, *be substrategies of S such that*

$$S_j = \{\boldsymbol{y} \in S \,|\, \mathfrak{P}_i(\boldsymbol{r}(\ \cdot\ ; (\boldsymbol{\beta}_0, \boldsymbol{\gamma}_0), \boldsymbol{y}))\}, \ \ \forall j \in \{1, 2\} \ \& \ S_3 = \{\boldsymbol{y} \in S \,|\, \neg \mathfrak{P}_1(\boldsymbol{r}(\ \cdot\ ; (\boldsymbol{\beta}_0, \boldsymbol{\gamma}_0), \boldsymbol{y}))\}.$$

Then

1. $S_1 \subseteq S_2$ *and*
2. $S_3 = S \smallsetminus S_1$.

For example, for a given $(\boldsymbol{\beta}_0, \boldsymbol{\gamma}_0) \in F(\mathcal{X}; \mathcal{P}_{tr,r})$ that satisfies (3) and a given $i \in \{1, ..., m\}$, the horizontal with respect to x_i substrategy of $\hat{S} = \hat{S}(\boldsymbol{\beta}_0, \boldsymbol{\gamma}_0)$ is the set-theoretic complement with respect to $\hat{S}$ of the x_i-based substrategy of $\hat{S}$. The scope of the present paper can be now stated as the comparison of the above substrategies for x_i being the age of an individual of a population.

2.2. Comparison of strategies

Here we introduce a scheme for the comparison of strategies, for which we need some preliminary notions, such as the basic reproductive number and the graded strategies.

2.2.1. $\mathcal{R}_0$: The measure of comparison

An important epidemiological notion studied and used extensively in the epidemiological literature is the basic reproductive number, $\mathcal{R}_0$, which is defined as the average number of infectious cases directly generated by one such case in a population where all individuals are susceptible to an infection. For every mathematical model, that describes a problem under study, corresponds a respective $\mathcal{R}_0$, which can be calculated with several ways, such as with the next-generation method or the existence of the endemic equilibrium (Diekmann & Heesterbeek, 2000).

In general, $\mathcal{R}_0$ depends on both the independent variables and the parameters of a model, therefore it is considered as a function defined as

$$\mathcal{R}_0 : \mathcal{X} \times F(\mathcal{X}; \mathcal{P}_{tr}, r) \times F(\mathcal{X}; \mathcal{P}_{other}) \to (0, \infty)$$
$$(\boldsymbol{x}, (\boldsymbol{\beta}, \boldsymbol{\gamma}), \boldsymbol{\delta}) \mapsto \mathcal{R}_0(\boldsymbol{x}, (\boldsymbol{\beta}, \boldsymbol{\gamma}), \boldsymbol{\delta}).$$

Only for the sake of brevity and compactness of the exposition, in the present paper we assume that it is independent of $\boldsymbol{x}$, that is

$$\mathcal{R}_0 : F(\mathcal{X}; \mathcal{P}_{tr}, r) \times F(\mathcal{X}; \mathcal{P}_{other}) \to (0, \infty)$$
$$((\boldsymbol{\beta}, \boldsymbol{\gamma}), \boldsymbol{\delta}) \mapsto \mathcal{R}_0((\boldsymbol{\beta}, \boldsymbol{\gamma}), \boldsymbol{\delta}).$$

In the proposed scheme, we check how one strategy measures against another of a special kind, via the calculation of the respective values of $\mathcal{R}_0$. That special kind of strategies is described below.

2.2.2. Gradable and graded strategies

The notion of the graded strategies is the crux of the proposed scheme. But before its introduction, we first need the following one.

Defintion 6.　(gradable strategy). *Let*

1. $(\boldsymbol{\beta}_0, \boldsymbol{\gamma}_0) \in F(\mathcal{X}; \mathcal{P}_{\text{tr,r}})$ *satisfy* (3) *and*
2. $S = S(\boldsymbol{\beta}_0, \boldsymbol{\gamma}_0)$ *be a respective strategy.*

We call S gradable iff $\forall \boldsymbol{\delta} \in F(\mathcal{X}; \mathcal{P}_{\text{other}})$ *the function* $\mathcal{R}_0|_S(\cdot, \boldsymbol{\delta})$ *is injective.*

Since $\mathcal{R}_0(S, \boldsymbol{\delta}) \subseteq (0, \infty)$, $\forall \boldsymbol{\delta} \in F(\mathcal{X}; \mathcal{P}_{\text{other}})$, we can arrange any family of pairwise distinct elements of such a set in a strictly ascending order when S is gradable, hence the following notion is well-defined.

Defintion 7.　(graded strategy). *Let*

1. $(\boldsymbol{\beta}_0, \boldsymbol{\gamma}_0) \in F(\mathcal{X}; \mathcal{P}_{\text{tr,r}})$ *satisfy* (3),
2. $S = S(\boldsymbol{\beta}_0, \boldsymbol{\gamma}_0)$ *be a respective gradable strategy,*
3. $\boldsymbol{\delta} \in F(\mathcal{X}; \mathcal{P}_{\text{other}})$ *and*
4. $\{\boldsymbol{y}_i\}_{i=1}^k \subseteq S$ *be a family of pairwise distinct elements of S, such that*

$$\underbrace{\mathcal{R}_0(\boldsymbol{y}_1, \boldsymbol{\delta})}_{=:G_1} < \ldots < \underbrace{\mathcal{R}_0(\boldsymbol{y}_k, \boldsymbol{\delta})}_{=:G_k}.$$

We call the pair $\left(S, \boldsymbol{G} = (G_i)_{i=1}^k\right)$ *a graded strategy, while* **G** *is called a gradation of S and each of the $G_1, \ldots, G_k$ is called a grade of* **G***.*

We note that the gradation of a graded strategy is a matter of choice. In what follows, for the sake of simplicity, we write S instead of $(S, \boldsymbol{G})$ for a graded strategy.

2.2.3. Comparison table and coverage

With the above toolbox at hand, we propose a scheme for the comparison of two strategies, only when one of them is graded. In addition, the scheme allows us to include many substrategies of the other strategy. Below, we present the steps required for the utilization of the proposed scheme, which is governed by the construction of the respective *comparison table* and analyzed in terms of *epidemiological* and *social coverage*.

Construction of the comparison table

1. Placing of the grades $G_1, \ldots, G_k$ of the gradation $\boldsymbol{G} = (G_i)_{i=1}^k$ of a given graded strategy S_1, in increasing order, to the top row:

2. Placing the under study substrategies $\{S_{2_i}\}_{i=1}^\ell$ of a second strategy S_2 to the left of the table, with the intent of comparing them against the first graded strategy.

3. Populating the comparison table with $\star$, where

$$\star_{ij} = \begin{cases} \checkmark & \text{if the } \mathcal{R}_0 \text{ of } S_{2i} \text{ is less than or equal to } G_j \\ \boldsymbol{\mathsf{X}} & \text{otherwise,} \end{cases} \quad \forall (i,j) \in \{1,\ldots,\ell\} \times \{1,\ldots,k\} .$$

S_2 \ S_1	G_1	G_2	$\cdots$	G_k
S_{2_1}	$\star_{11}$	$\star_{12}$	$\cdots$	$\star_{1k}$
S_{2_2}	$\star_{21}$	$\star_{22}$	$\cdots$	$\star_{2k}$
$\vdots$	$\vdots$	$\vdots$	$\ddots$	$\vdots$
S_{2_ℓ}	$\star_{\ell 1}$	$\star_{\ell 2}$	$\cdots$	$\star_{\ell k}$

Next, we present two ways to read the comparison table for extracting useful information.

Social overview of the comparison table: epidemiological coverage. Here we compare S_2 to S_1. In particular, for every fixed substrategy of S_2 (social overview), we check how good of an alternative it is, compared to S_1 (epidemiological coverage).

$4_\rightarrow$. Calculating the epidemiological coverage of the gradation $\boldsymbol{G}$ of S_1 by each substrategy of S_2, by calculating the average number of $\checkmark$ in each row.

S_2 \ S_1	G_1	G_2	$\cdots$	G_k	Epidemiological coverage $(\cdot 100\%)$
S_{2_1}	$\star_{11}$	$\star_{12}$	$\cdots$	$\star_{1k}$	$\frac{\#\{\star_{1j}=\checkmark\}_{j=1}^k}{k}$
S_{2_2}	$\star_{21}$	$\star_{22}$	$\cdots$	$\star_{2k}$	$\frac{\#\{\star_{2j}=\checkmark\}_{j=1}^k}{k}$
$\vdots$	$\vdots$	$\vdots$	$\ddots$	$\vdots$	$\vdots$
S_{2_ℓ}	$\star_{\ell 1}$	$\star_{\ell 2}$	$\cdots$	$\star_{\ell k}$	$\frac{\#\{\star_{\ell j}=\checkmark\}_{j=1}^k}{k}$

$5_\rightarrow$. Calculating the total coverage of the gradation $\boldsymbol{G}$ of S_1 by the whole S_2, through the average value of all epidemiological coverages.

S_2 \ S_1	G_1	G_2	$\cdots$	G_k	Epidemiological coverage $(\cdot 100\%)$
S_{2_1}	$\star_{11}$	$\star_{12}$	$\cdots$	$\star_{1k}$	$\frac{\#\{\star_{1j}=\checkmark\}_{j=1}^k}{k}$
S_{2_2}	$\star_{21}$	$\star_{22}$	$\cdots$	$\star_{2k}$	$\frac{\#\{\star_{2j}=\checkmark\}_{j=1}^k}{k}$
$\vdots$	$\vdots$	$\vdots$	$\ddots$	$\vdots$	$\vdots$
S_{2_ℓ}	$\star_{\ell 1}$	$\star_{\ell 2}$	$\cdots$	$\star_{\ell k}$	$\frac{\#\{\star_{\ell j}=\checkmark\}_{j=1}^k}{k}$
					$\frac{\#\{\star_{ij}=\checkmark\}_{i,j=1}^{\ell,k}}{\ell \cdot k}$

The takeaway of the above analysis is that if the total (epidemiological) coverage of $\boldsymbol{G}$ by the (respective sub-)strategy S_2 (S_{2_i}, for $i \in \{1,\ldots,\ell\}$) is satisfying, then S_2 (S_{2_i}) could be considered as an alternative to S_1. We note that the quantification of the term "satisfying" is subjective.

Epidemiological overview of the comparison table: social coverage. Here we compare S_1 to S_2. In particular, for every fixed grade of $\boldsymbol{G}$ (epidemiological overview), we check how much of that grade S_2 is (social coverage).

$4_\downarrow$. Calculating the social coverage of S_2 by each grade of $\boldsymbol{G}$ of S_1, by calculating the average number of in each column.

S_2 \ S_1	G_1	G_2	$\cdots$	G_k	
S_{2_1}	$\star_{11}$	$\star_{12}$	$\cdots$	$\star_{1k}$	
S_{2_2}	$\star_{21}$	$\star_{22}$	$\cdots$	$\star_{2k}$	
$\vdots$	$\vdots$	$\vdots$	$\ddots$	$\vdots$	
S_{2_ℓ}	$\star_{\ell 1}$	$\star_{\ell 2}$	$\cdots$	$\star_{\ell k}$	
Social coverage ($\cdot 100\%$)	$\dfrac{\#\{\star_{i1}=\checkmark\}_{i=1}^{\ell}}{\ell}$	$\dfrac{\#\{\star_{i2}=\checkmark\}_{i=1}^{\ell}}{\ell}$	$\cdots$	$\dfrac{\#\{\star_{ik}=\checkmark\}_{i=1}^{\ell}}{\ell}$	[shaded]

$5_\downarrow$. Calculating the total coverage of S_2 by the whole $\boldsymbol{G}$ of S_1, through the average value of all social coverages.

S_2 \ S_1	G_1	G_2	$\cdots$	G_k	
S_{2_1}	$\star_{11}$	$\star_{12}$	$\cdots$	$\star_{1k}$	
S_{2_2}	$\star_{21}$	$\star_{22}$	$\cdots$	$\star_{2k}$	
$\vdots$	$\vdots$	$\vdots$	$\ddots$	$\vdots$	
S_{2_ℓ}	$\star_{\ell 1}$	$\star_{\ell 2}$	$\cdots$	$\star_{\ell k}$	
Social coverage ($\cdot 100\%$)	$\dfrac{\#\{\star_{i1}=\checkmark\}_{i=1}^{\ell}}{\ell}$	$\dfrac{\#\{\star_{i2}=\checkmark\}_{i=1}^{\ell}}{\ell}$	$\cdots$	$\dfrac{\#\{\star_{ik}=\checkmark\}_{i=1}^{\ell}}{\ell}$	$\dfrac{\#\{\star_{ij}=\checkmark\}_{i,j=1}^{\ell,k}}{\ell\cdot k}$

Total overview of the comparison table. Here, we combine the social and the epidemiological overview of the comparison table.

6. Merging of the social and epidemiological overviews.

S_2 \ S_1	G_1	G_2	$\cdots$	G_k	Epidemiological coverage ($\cdot 100\%$)
S_{2_1}	$\star_{11}$	$\star_{12}$	$\cdots$	$\star_{1k}$	$\dfrac{\#\{\star_{1j}=\checkmark\}_{j=1}^{k}}{k}$
S_{2_2}	$\star_{21}$	$\star_{22}$	$\cdots$	$\star_{2k}$	$\dfrac{\#\{\star_{2j}=\checkmark\}_{j=1}^{k}}{k}$
$\vdots$	$\vdots$	$\vdots$	$\ddots$	$\vdots$	$\vdots$
S_{2_ℓ}	$\star_{\ell 1}$	$\star_{\ell 2}$	$\cdots$	$\star_{\ell k}$	$\dfrac{\#\{\star_{\ell j}=\checkmark\}_{j=1}^{k}}{k}$
Social coverage ($\cdot 100\%$)	$\dfrac{\#\{\star_{i1}=\checkmark\}_{i=1}^{\ell}}{\ell}$	$\dfrac{\#\{\star_{i2}=\checkmark\}_{i=1}^{\ell}}{\ell}$	$\cdots$	$\dfrac{\#\{\star_{ik}=\checkmark\}_{i=1}^{\ell}}{\ell}$	$\dfrac{\#\{\star_{ij}=\checkmark\}_{i,j=1}^{\ell,k}}{\ell\cdot k}$

3. Horizontal lockdowns versus age-based interventions

In this section, we investigate whether age-based interventions can offer a replacement to horizontal lockdowns for the case of SARS-CoV-2, following the framework presented in §2, and using the model studied in Bitsouni et al. (2024), which is presented in Appendix A. In §3.1, we categorize the parameters into δ, β and γ, and pick our choice of strategic scales, $\boldsymbol{r}$; both (β, γ) and $\boldsymbol{r}$ serve for the definition of the strategies under investigation. Additionally, we distribute the total population of $\mathscr{P}$ (4) into five cohorts, based on age, θ, of each individual. In §3.3, we define the graded strategy of horizontal lockdowns and the strategy of age-based restrictions. Finally, in §3.4, we compare the aforementioned strategies.

3.1. Choice of general strategy

The independent variables that appear in $\mathscr{P}$ (4) are t and θ, thus

$$\boldsymbol{x} = (t, \theta).$$

In order to define the strategies under investigation, we need to categorize the parameters appeared in $\mathscr{P}$ (4) into $(\boldsymbol{\beta}_0, \boldsymbol{\gamma}_0)$ and $\boldsymbol{\delta}$, and consequently choose an appropriate strategic scale as discussed in §2.1.

The parameters which affect the strategies under investigation are β_A, β_I and γ_I. Therefore, we have that

$$(\boldsymbol{\beta}_0, \boldsymbol{\gamma}_0) = (\beta_A, \beta_I, \gamma_I),$$

whereas

$$\boldsymbol{\delta} = (\mu, p, \epsilon, \zeta, k, q, \xi, \chi, \gamma_A),$$

with the parameter values being as in Table 1.

We note that regardless of the seemingly important role of asymptomaticity (see Appendix A) for the spread of the disease, the performance of the means of detection, such as the rapid antigen tests (Ag-RDTs), for the case of asymptomatic infectious individuals still remains ambiguous (Centers for Disease Control and Prevention, 2020; Pollock & Lancaster, 2020; SAGE 56th meeting on COVID-19, 2020; Soni et al., 2023). In the light of the above we prefer not to incorporate such means to our general strategy, hence we exclude γ_A from $(\boldsymbol{\beta}_0, \boldsymbol{\gamma}_0)$. Moreover, we note that (3) holds.

We are now ready to construct our choice of general strategy along with its strategic scales, following the next steps.

1. We consider an interval $\Lambda \subseteq \mathbb{R}_0^+$ such that $0 \in \Lambda$, to be the average lifespan of an individual of the population under study, hence $\theta \in \Lambda$. Of course, $\sup \Lambda < \infty$.
2. We discretize Λ by considering a respective partition $\Delta_\Lambda := \{\delta_j\}_{j=0}^n$, for a fixed $n \in \mathbb{N}$, i.e.,

$$0 = \delta_0 < \delta_1 < \ldots < \delta_n = \sup \Lambda$$

and we define the subintervals

$$\Lambda_j := [\delta_{j-1}, \delta_j), \quad \forall j \in \{1, \ldots, n\}.$$

3. We set

$$\Lambda_W := \bigcup_{j \in W} \Lambda_j, \quad \forall W \in \mathcal{P}(\{1, \ldots, n\}),$$

where $\mathcal{P}$ stands for the power set, as well as we define

Table 1

A list of parameters of $\mathscr{M}$, along with their value, units, and value source. For their derivation, see Appendix B.

Parameters	Value	Units	Source
N_0	$80 \cdot 10^6$	individuals	Estimated from Mathieu et al. (2020)
μ	$4.38356 \cdot 10^{-5}$	day^{-1}	Estimated from Mathieu et al. (2020)
β_A	Fig. 13	individual$^{-1} \cdot$ day^{-1}	Estimated from Del Valle et al. (2007)
β_I	Fig. 13	individual$^{-1} \cdot$ day^{-1}	Estimated from Del Valle et al. (2007)
p	10^{-3}	day^{-1}	Estimated from Mathieu et al. (2020)
ϵ	0.7	—	Estimated from Grant et al. (2022)
ζ	$\frac{1}{14}$	day^{-1}	Estimated from Chau et al. (2022)
k	Equation 6	day^{-1}	Estimated from Kang et al. (2022), Wu et al. (2022)
q	Fig. 14	—	Estimated from Sah et al. (2021)
ξ	0.5	—	Estimated from He et al. (2021), Buitrago-Garcia et al. (2022)
χ	Equation 7	day^{-1}	Estimated from He et al. (2021), Buitrago-Garcia et al. (2022)
γ_A	$\frac{1}{8}$	day^{-1}	Estimated from Byrne et al. (2020)
γ_I	$\frac{1}{14}$	day^{-1}	Estimated from Byrne et al. (2020)

$$\rho_W(\,\cdot\,;a):\ \Lambda\to[0,1]$$

$$\theta\mapsto\rho_W(\theta;a):=\begin{cases}1 & \theta\notin\Lambda_W \\[2mm] a & \theta\in\Lambda_W,\end{cases}\quad\forall(W,a)\in\mathcal{P}(\{1,\dots,n\})\times[0,1)$$

and

$$g_W(\,\cdot\,;b):\ \Lambda\to[1,\infty]$$

$$\theta\mapsto g_W(\theta;b):=\begin{cases}1 & \theta\notin\Lambda_W \\[2mm] \dfrac{1}{b} & \theta\in\Lambda_W,\end{cases}\quad\forall(W,b)\in\mathcal{P}(\{1,\dots,n\})\times[0,1),$$

where the choice of $(a,b)\in[0,1)^2$ is left to be explained.

We note that in the extreme cases of $W\in\{\varnothing,\{1,\dots,n\}\}$ we have $\Lambda_\varnothing=\varnothing$ and $\Lambda_{\{1,\dots,n\}}=\Lambda$, as well as

$$(\rho_\varnothing(\,\cdot\,;a),g_\varnothing(\,\cdot\,;b))=(1,1),\ \forall(a,b)\in[0,1)^2$$

and

$$\left(\rho_{\{1,\dots,n\}}(\,\cdot\,;a),g_{\{1,\dots,n\}}(\,\cdot\,;b)\right)=\left(a,\frac{1}{b}\right),\ \forall(a,b)\in[0,1)^2.$$

Hence, the above functions are independent of θ iff $W\in\{\varnothing,\{1,\dots,n\}\}$, as well as they are equal to 1 iff $W=\varnothing$.

4. We define the strategic scales to be

$$\boldsymbol{r}_{W_\beta,W_\gamma}(\,\cdot\,;a,b):=\left(\rho_{W_\beta}(\,\cdot\,;a),\rho_{W_\beta}(\,\cdot\,;a),g_{W_\gamma}(\,\cdot\,;b)\right),\quad\forall(W_\beta,W_\gamma,a,b)\in(\mathcal{P}(\{1,\dots,n\}))^2\times[0,1)^2.$$

5. The general strategy of interest S has the form

$$S:=\left\{(\beta,\gamma)=\boldsymbol{r}_{W_\beta,W_\gamma}(\,\cdot\,;a,b)\odot(\beta_0,\gamma_0)\,\Big|\,(W_\beta,W_\gamma,a,b)\in(\mathcal{P}(\{1,\dots,n\}))^2\times[0,1)^2\right\}.$$

Regarding $a\in[0,1]$, in the light of (1), the effect of every $\rho_{W_\beta}(\,\cdot\,,a)$ to β can be interpreted as having the average number of close contacts of an (asymptomatic or symptomatic) infectious individual belonging to Λ_{W_β} reduced by $1-a$, i.e.

$$(c_A,c_I)|_{\Lambda_{W_\beta}}\mapsto a\cdot(c_A,c_I)|_{\Lambda_{W_\beta}}$$

Regarding $b\in(0,1]$, in the light of (2), the effect of every $g_{W_\gamma}(\,\cdot\,,b)$ to γ can be interpreted as having the average period an individual belonging to Λ_{W_β} spends on compartment I before moving into compartment R reduced by $1-b$, i.e.

$$P_{I\to R}|_{\Lambda_{W_\beta}}\mapsto b\cdot P_{I\to R}|_{\Lambda_{W_\beta}}$$

3.2. Choice of distribution of the population into age cohorts

We now specify the distribution of the whole population into cohorts with respect to the age of each individual, hence with respect to its occupational and social activity.

We divide the population into five (5) cohorts, thus $n=5$, as seen in Fig. 2, where $\Lambda=[0,90)$ years and $\Delta_\Lambda=\{0,6,18,24,65,90\}$ years (both non-scaled). The 1st cohort is made of toddlers and preschoolers, the 2nd is made of school students, the 3rd is primarily made of university students, the 4th is primarily made of the working class, and the 5th is primarily made of pensioners.
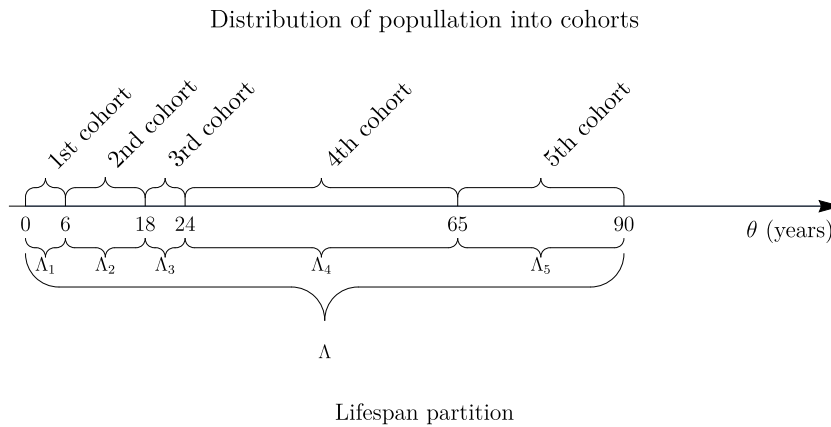
Distribution of popullation into cohorts

Fig. 2. The partition of the non-scaled lifespan and the respective distribution of the whole population into cohorts. The partition was made by taking into account the social profile connecting individuals in each cohort, such as going to school, working, or being pensioners.

As an example of the strategic scale within the context of the cohorts presented in Fig. 2, the reduction of the number of contacts of the 1st and 3rd cohort by 80% and not performing tests on any cohort is modeled by the strategic scale

$$\boldsymbol{r}_{\{1,3\},\varnothing}\left(\,\cdot\,;\frac{1}{5},\,\cdot\,\right) = \left(\rho_{\{1,3\}}\left(\,\cdot\,;\frac{1}{5}\right), g_{\varnothing}(\,\cdot\,;\,\cdot\,)\right),$$

where

$$\rho_{\{1,3\}}\left(\theta;\frac{1}{5}\right) = \begin{cases} \frac{1}{5}, & \text{if } \theta \in \Lambda_1 \\ 1, & \text{if } \theta \in \Lambda_2 \\ \frac{1}{5}, & \text{if } \theta \in \Lambda_3 \\ 1, & \text{if } \theta \in \Lambda_4 \\ 1, & \text{if } \theta \in \Lambda_5, \end{cases}$$

and

$$g_{\varnothing}(\theta;\,\cdot\,) = 1, \ \forall \theta \in \Lambda.$$

3.3. Choice of substrategies of general strategy

In this section, we define the two strategies under investigation. Furthermore, we utilize the strategic scale introduced in §3.1 to model each strategy.

3.3.1. Horizontal lockdowns substrategy

It is straightforward to check that the largest horizontal with respect to age substrategy of S is

$$\left\{ (\boldsymbol{\beta},\gamma) = \boldsymbol{r}_{W_\beta,W_\gamma}(\,\cdot\,;a,b) \odot (\boldsymbol{\beta}_0,\gamma_0) \,\middle|\, (W_\beta, W_\gamma, a, b) \in (\mathcal{P}(\{1,\ldots,5\}))^2 \times [0,1)^2 \quad \text{such that } (W_\beta, W_\gamma) \in \{\varnothing, \{1,\ldots,5\}\}^2 \right\},$$

which implies that every substrategy of the above strategy is horizontal with respect to age.

Thus, a choice of horizontal lockdowns substrategy can be made by considering $S_1 \subseteq S$ as

$$S_1 = \left\{ (\boldsymbol{\beta},\gamma) = \boldsymbol{r}_{\{1,\ldots,5\},\varnothing}(\,\cdot\,;a,\,\cdot\,) \odot (\boldsymbol{\beta}_0,\gamma_0) \,\middle|\, a \in [0,1) \right\}.$$

The intensity (that is the amount of contact reduction for every individual) can be varied but uniformly, that is,

$$a \in [0,1) \quad \text{and} \quad W_\beta = \{1,\ldots,n\},$$

respectively, in order to capture different scenarios. We also assume that no tests are performed in any of the five cohorts, i.e.

$W_\gamma = \varnothing.$

Now, S_1 is gradable, since from (5) we get that

$$\mathcal{R}_0(\boldsymbol{\beta}, \gamma, \boldsymbol{\delta}) = a \cdot \mathcal{R}_0(\boldsymbol{\beta}_0, \gamma_0, \boldsymbol{\delta}), \, \forall (\boldsymbol{\beta}, \gamma) \in S_1.$$

In particular, $\mathcal{R}_0$ is strictly increasing with respect to a, as it is depicted in Table 2.

To get a better understanding of how $a \in [0, 1)$ translates into the real life intensity of a stay-at-home restriction policy, we firstly notice that when $W_\beta = \varnothing$ (or else $a \to 1^-$), we have that no stay-at-home restrictions are in effect. In that case, our model predicts an $\mathcal{R}_0$ of 2.854 (or else $\mathcal{R}_0 \to 2.854^-$), which is in line with various systematic reviews found in scientific literature, such as 2.87 (95% CI: 2.39−3.44) in Billah et al. (2020) and 2.69 (95% CI: 2.40−2.98) in Ahammed et al. (2021), which solidifies the validity of our model in predicting the $\mathcal{R}_0$ of SARS-CoV-2 pandemic. Furthermore, we see that the tight lock-down Italy enforced in early 2020 resulted in an 82% reduction in mobility (Vinceti et al., 2022), which would correspond to a being approximately equal to 0.2. During the same time frame in Germany, the authors of Schlosser et al. (2020), report about a 50% drop in the average number of contacts, which corresponds to $a = 0.5$. Finally, in Zhou et al. (2020) the authors show that even a 20% reduction in mobility proved a good way of delaying the spread of the infection, which would correspond to a being approximately equal to 0.8.

Based on the aforementioned cases, we construct three different scenarios based on the intensity of the mobility restrictions:

- the low intensity scenario, $\mathcal{L}$, where the average number of contacts is reduced by 20% and $\mathcal{R}_{0\mathcal{L}} = 2.283$,
- the medium intensity scenario, $\mathcal{M}$, where the average number of contacts is reduced by 50% and $\mathcal{R}_{0\mathcal{M}} = 1.427$ and
- the high intensity scenario, $\mathcal{H}$, where the average number of contacts is reduced by 80% and $\mathcal{R}_{0\mathcal{H}} = 0.571$.

The above scenarios constitute a gradation $\boldsymbol{G}$ of S_1 with

$$G_1 = \mathcal{R}_{0\mathcal{H}}, \; G_2 = \mathcal{R}_{0\mathcal{M}} \text{ and } G_3 = \mathcal{R}_{0\mathcal{L}}.$$

Such a gradation is summarized in Table 3.

3.3.2. Aged-based substrategies

The largest aged-based substrategy of S, $S_2 \subseteq S$, is

$$S_2 = \left\{ \left(\boldsymbol{\beta}, \gamma\right) = \boldsymbol{r}_{W_\beta, W_\gamma}(\cdot; a, b) \odot (\boldsymbol{\beta}_0, \gamma_0) \, \middle| \, (W_\beta, W_\gamma, a, b) \in (\mathcal{P}(\{1, \ldots, 5\}))^2 \times [0, 1)^2 \text{ such that } (W_\beta, W_\gamma) \notin \{\varnothing, \{1, \ldots, 5\}\}^2 \right\},$$

Table 2
The value of $\mathcal{R}_0$ decreases linearly as the intensity of the stay-at-home restrictions increases, i.e. as a decreases.

a	Contact reduction	$\mathcal{R}_0$
0	100%	0
0.1	90%	0.285
0.2	80%	0.571
0.3	70%	0.856
0.4	60%	1.141
0.5	50%	1.427
0.6	40%	1.712
0.7	30%	1.998
0.8	20%	2.283
0.9	10%	2.569

Table 3
Summary of the three horizontal lockdowns' intensity scenarios, Low ($\mathcal{L}$), Medium ($\mathcal{M}$) and High ($\mathcal{H}$), which constitute a gradation of S_1.

Gradation	Intensity level	Contact reduction	$\mathcal{R}_0$
G_1	High ($\mathcal{H}$)	80%	0.571
G_2	Medium ($\mathcal{M}$)	50%	1.427
G_3	Low ($\mathcal{L}$)	20%	2.283

Table 4

The sixteen age-based substrategies $\{S_{2_i}\}_{i=1}^{16}$ of S_2 which are chosen for the comparison to S_1.

i	Age-based interventions	W_β	W_γ
1	Contact reduction: 1st, 2nd, 3rd cohorts Testing: 4th, 5th cohorts	$\{1,2,3\}$	$\{4,5\}$
2	Contact reduction: 4th, 5th cohorts Testing: 1st, 2nd, 3rd cohorts	$\{4,5\}$	$\{1,2,3\}$
3	Contact reduction: 1st cohort Testing: 4th, 5th cohorts	$\{1\}$	$\{4,5\}$
4	Contact reduction: 4th, 5th cohorts Testing: 1st cohort	$\{4,5\}$	$\{1\}$
5	Contact reduction: 2nd cohort Testing: 4th, 5th cohorts	$\{2\}$	$\{4,5\}$
6	Contact reduction: 4th, 5th cohorts Testing: 2nd cohort	$\{4,5\}$	$\{2\}$
7	Contact reduction: 3rd cohort Testing: 4th, 5th cohorts	$\{3\}$	$\{4,5\}$
8	Contact reduction: 4th, 5th cohorts Testing: 3rd cohort	$\{4,5\}$	$\{3\}$
9	Contact reduction: 1st cohort Testing: 2nd cohort	$\{1\}$	$\{2\}$
10	Contact reduction: 2nd cohort Testing: 1st cohort	$\{2\}$	$\{1\}$
11	Contact reduction: 4th cohort Testing: 5th cohort	$\{4\}$	$\{5\}$
12	Contact reduction: 5th cohort Testing: 4th cohort	$\{5\}$	$\{4\}$
13	Contact reduction: 2nd cohort Testing: 4th cohort	$\{2\}$	$\{4\}$
14	Contact reduction: 4th cohort Testing: 2nd cohort	$\{4\}$	$\{2\}$
15	Contact reduction: 2nd cohort Testing: 5th cohort	$\{2\}$	$\{5\}$
16	Contact reduction: 5th cohort Testing: 2nd cohort	$\{5\}$	$\{2\}$

which implies that every substrategy of S_2 is aged-based hence it can potentially be compared to the graded S_1. For our simulations, we choose the substrategies $\{S_{2_i}\}_{i=1}^{16}$ of S_2 summarized in Table 4 for the comparison to S_1.

3.4. Simulations and results

Here we employ the scheme introduced in §2.2 for the comparison between S_1 of §3.3.1 and $\{S_{2_i}\}_{i=1}^{16}$ of §3.3.2. The simulations were performed using Mathematica 13.1 (Wolfram Research Inc., 2022). In the end of this section, we summarize its results with the comparison table.

3.4.1. Social overview of the results, S_2 versus S_1

Throughout our simulations, we let the (a, b) of each strategic scale to take values in the 2D interval $[0, 1)^2$ and illustrate the results in density plots, where in the x-axis and y-axis we have $a \cdot 100\%$ and $b \cdot P_{I \to R} = \frac{b}{\gamma_I} = b \cdot 14$ days, respectively.

$S_{2_{1,2}}$ **versus** S_1. We begin by examining whether restrictions on the younger or the older cohorts play a more important role in reducing $\mathcal{R}_0$. In Fig. 3a, we see that in order to achieve the same $\mathcal{R}_0$ as the scenario $\mathcal{H}$, the contact reduction of the first three cohorts needs to be at least 75% and the individuals of the last two cohorts need to be detected and removed at least before the twelfth day. Additionally, since the absolute value of the gradient of the contour lines is high, the younger cohorts influence the dynamics of $\mathcal{R}_0$ more when compared to the older cohorts. In Fig. 3b, we see that the scenario $\mathcal{H}$, can be replaced by finding and removing from the community the people belonging in the first three cohorts at around the third day from symptom onset, whereas the contact reduction of the older age cohorts is almost irrelevant. Furthermore, since the gradient of the contour lines is almost zero, the younger cohorts play a far greater role in reducing $\mathcal{R}_0$ when compared to the older cohorts, especially the more austere the restrictions are. Overall, Fig. 3 shows us that the younger cohorts are more influential in the dynamics of $\mathcal{R}_0$, both when they are faced with social distancing restrictions, and with mandatory testing.

It is now clear that the younger cohorts play a far more important role in the dynamics of $\mathcal{R}_0$. We subsequently examine whether similar results as those presented in Fig. 3 can be achieved, by restricting just one of the three younger cohorts instead of all three of them together.

$S_{2_{3,4}}$ **versus** S_1. Fig. 4 illustrates restrictions on the 1st and the 4th − 5th cohorts. When social distancing on the 1st cohort and testing on the 4th and 5th cohorts are enforced, scenario $\mathcal{M}$ can only be achieved with the strongest possible restrictions on the aforementioned cohorts, as we can see in Fig. 4a. When the restrictions on the cohorts are reversed, Fig. 4b shows that
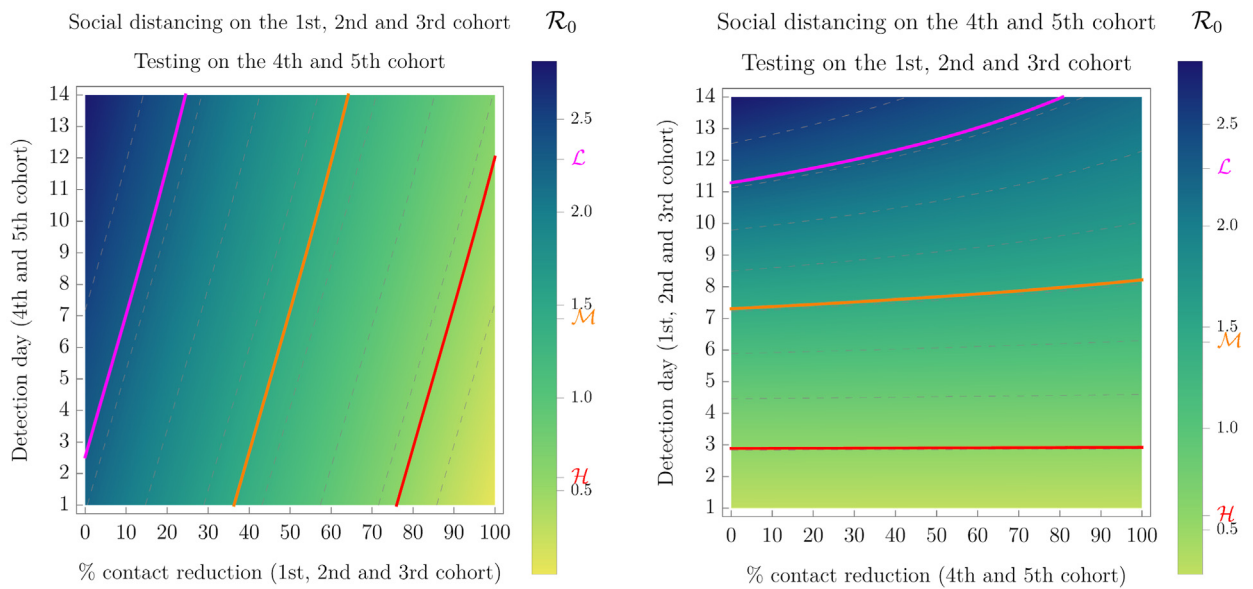
(a) $\mathcal{R}_0$ when social distancing is enforced on the 1st, 2nd and 3rd cohort and testing is enforced on the 5th and 6th cohort ($W_{\boldsymbol{\beta}} = \{1, 2, 3\}$ and $W_{\gamma} = \{4, 5\}$).

(b) $\mathcal{R}_0$ when social distancing is enforced on the 5th and 6th cohort and testing is enforced on the 1st, 2nd and 3rd cohort ($W_{\boldsymbol{\beta}} = \{5, 6\}$ and $W_{\gamma} = \{1, 2, 3\}$).

Fig. 3. Two density plots of the grouping of the three younger cohorts and the two older cohorts together. In both cases, all three of our horizontal lockdown scenarios $\mathcal{L}, \mathcal{M}$ and $\mathcal{H}$, can be replaced by enforcing a wide range of intensity level restrictions to the different cohort groupings.

scenario $\mathcal{H}$ can be achieved if the day that the symptomatic infectious individuals are detected and removed from the community is around the second day, with the contact reduction of the 4th and 5th cohort being almost irrelevant just like the case described by Fig. 3. There is, however, a one-day difference in the required detection day of asymptomatic individuals between the scenarios presented in Fig. 3b and Fig. 4b for them to have the same effect on R_0, as scenario $\mathcal{H}$. In other words, the procedure of detection and removal of asymptomatic individuals from the community needs to be one day faster when only the 1st cohort is getting tested when compared to the grouping of the 1st, 2nd and 3rd cohorts, for them to have the same results on $\mathcal{R}_0$ as scenario $\mathcal{H}$.

$S_{2_{5,6}}$ **versus** S_1. Next, we examine the importance of the 2nd cohort to the dynamics of $\mathcal{R}_0$, with the results being shown in Fig. 5. Contrary to the simulation of Fig. 4a, when social distance is enforced on the 2nd cohort, the results of scenario $\mathcal{M}$ can be achieved with far less strict policies. In particular, as shown in Fig. 5a, for scenario $\mathcal{M}$ to be achieved, the contacts of the 2nd cohort need to be reduced by at least 80% and the symptomatic individuals of the 4th and 5th cohorts need to be detected and removed from the community at least before around the fifth day. When the 2nd cohort is the one being tested, Fig. 5b shows that scenario $\mathcal{M}$ can be achieved by removing symptomatic individuals from the community at around the fifth day, with the reduction in the average number of contacts of the 4th and 5th cohorts being almost irrelevant, much like the simulations illustrated in Fig. 3b and Fig. 4b. Additionally, none of the simulations of Fig. 5 can act as a replacement measure to scenario $\mathcal{H}$.

$S_{2_{7,8}}$ **versus** S_1. Subsequently, we examine the contribution of the 3rd cohort to the dynamics of $\mathcal{R}_0$, with Fig. 6 illustrating the results. As we can see from Fig. 6, the 3rd cohort, in combination with the grouping of the 4th and 5th cohort, seems to influence the reduction of $\mathcal{R}_0$ far less when compared to the younger cohorts. The only horizontal lockdown scenario that can be replaced with this combination of age-based interventions is scenario $\mathcal{L}$. Additionally, even though the 1st and 2nd cohort dominated the dynamics of $\mathcal{R}_0$ when the symptomatic individuals of those cohorts were getting tested, that is not the case with the 3rd cohort, as can be seen from Fig. 6b. The same holds for the case when social distancing is enforced on the 3rd cohort, since the absolute value of the gradient of the contour lines of Fig. 6a is about 2. Hence, out of the three younger cohorts, the 3rd one has the weakest influence on the dynamics of $\mathcal{R}_0$.

$S_{2_{9,10}}$ **versus** S_1. The 1st and 2nd cohort seem to be the two cohorts that influence the dynamics of $\mathcal{R}_0$ the most. Hence, we quantify the results of targeting only the aforementioned cohorts in Fig. 7. As we can see from Fig. 7, all three horizontal lockdown scenarios $\mathcal{L}, \mathcal{M}$ and $\mathcal{H}$ can be replaced with a combination of measures targeted at the 1st and 2nd cohort. This particular combination of age-based measures has similar dynamics as the scenarios presented in Fig. 3 which combine all of our cohorts, and Fig. 4b which includes measures regarding three different cohorts. The vital role of the 1st and 2nd cohort is now undeniable. In Fig. 7a we see, that scenario $\mathcal{H}$ can be replaced with the contacts of the 1st cohort being reduced by at least
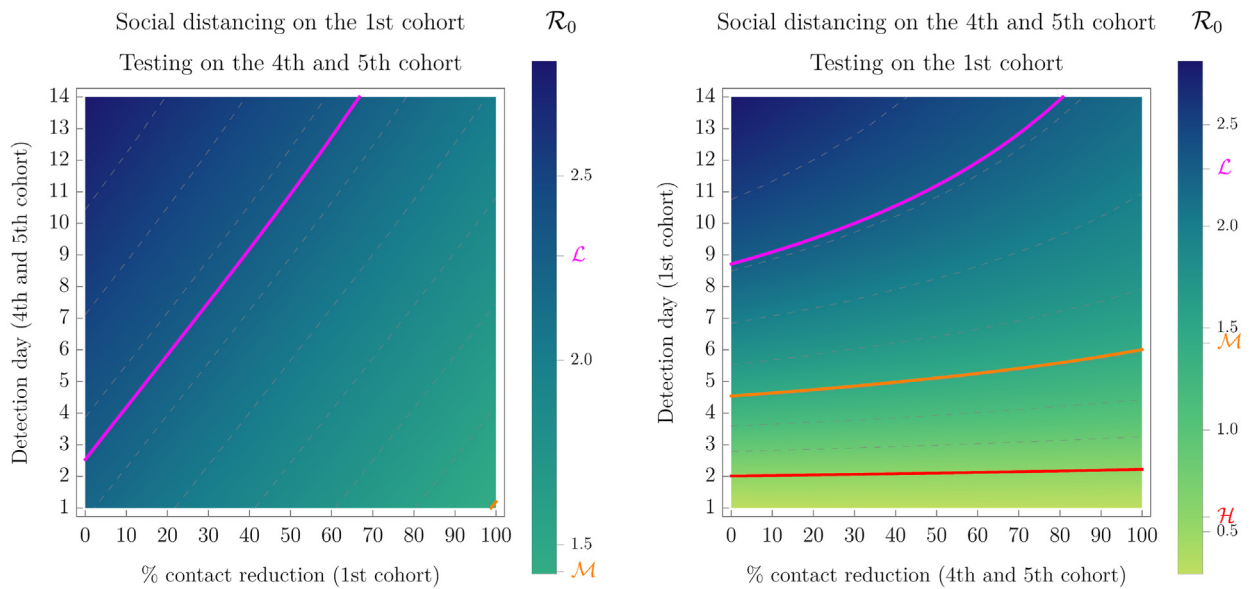
(a) $\mathcal{R}_0$ when social distancing is enforced on the 1st cohort and testing is enforced on the 5th and 6th cohort ($W_\beta = \{1\}$ and $W_\gamma = \{4, 5\}$).
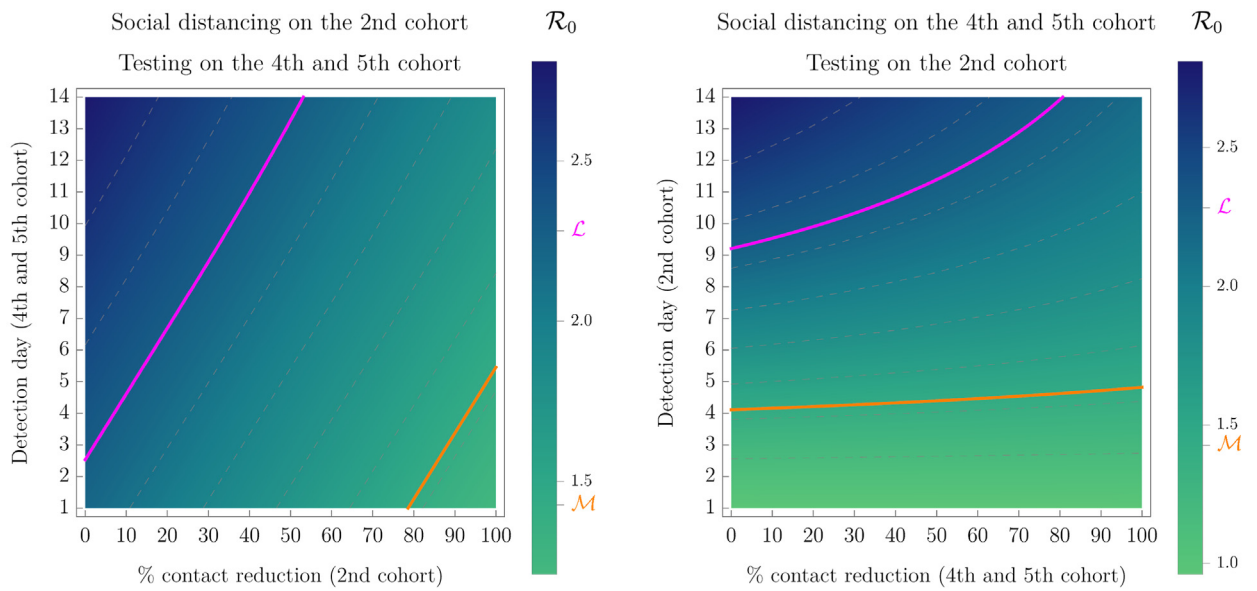
(b) $\mathcal{R}_0$ when social distancing is enforced on the 5th and 6th cohort and testing is enforced on the 1st cohort ($W_\beta = \{5, 6\}$ and $W_\gamma = \{1\}$).

Fig. 4. Two density plots of the 1st cohort and the grouping of the two older cohorts together. When social distancing is enforced on the 1st cohort scenario $\mathcal{H}$ can only be achieved when the most austere restriction are enforced. On the other hand, when the symptomatic individuals of the 1st cohort are the ones getting tested all three of our horizontal lockdown scenarios $\mathcal{L}, \mathcal{M}$ and $\mathcal{H}$, can be replaced by enforcing a wide range of intensity level restrictions to the 1st cohort and the grouping of the 4th and 5th cohort. The detection-and-removal day of asymptomatic individuals needs to be one day faster when compared to the simulation illustrated in Fig. 4b, for the same results as scenario $\mathcal{H}$ to apply.

50% and the infectious individuals of the 2nd cohort being found and removed from the community at least before the 4th day. When the restrictions are reversed, scenario $\mathcal{H}$ can be replaced when the symptomatic individuals of the 1st cohort are detected and removed from the community at around the second day after symptom onset, as can be seen in Fig. 7b, with minimal contribution from the 2nd cohort.

$S_{2_{11,12}}$ **versus S_1.** Up until now, we examined the two older cohorts, namely the 4th and 5th cohort, grouping them together as a single cohort. In an attempt to study the result of the interactions of the aforementioned cohorts individually, we present Fig. 8. As expected, from the inability of the grouping of the 4th and 5th cohort to dominate the dynamics of our previous simulations, the simulations of Fig. 8 offer a poor reduction of $\mathcal{R}_0$. Neither in Fig. 8a nor Fig. 8b can horizontal lockdown scenarios $\mathcal{H}$ and $\mathcal{M}$ be replaced by a combination of measures in the 4th and 5th cohort. Only scenario $\mathcal{L}$ can be replaced, and that is with austere restrictions on the 5th cohort. In particular, scenario $\mathcal{L}$ can be achieved either when the reduction of the average amount of contacts of the 4th cohort is 80% or when the symptomatic individuals of the 4th cohort are detected and removed from the community at around 2.5 days after symptom onset. Finally, there is a clear domination of the 4th cohort in this particular combination of age-based measures, with the measures enforced on the 5th cohort being irrelevant.

$S_{2_{13,14,15,16}}$ **versus S_1.** Lastly, we present the final combination of measures in Fig. 9. This final set of restrictions acts as a viable proposal to a real life situation with the economic impact of the measures in mind, since it targets the 2nd cohort, i.e., school students, whose contact reduction, or in other words school closures, would minimally affect the economy. Additionally, Fig. 9, allows us to examine the difference between the grouping of the two older cohorts and their individual contribution to $\mathcal{R}_0$, in combination to another, younger, cohort. As can be seen in Fig. 9a, for horizontal lockdown scenario $\mathcal{M}$ to be replaced, the contact reduction of the 2nd cohort needs to be at least 85% and the infectious individuals of the 4th cohort need to be found and removed from the community at least before the fourth day after symptom onset. Compared to Fig. 5a, there is a 5% increase in the required contact reduction for scenario $\mathcal{M}$ to be replaced, as well as about a 1.5 day decrease between the required detection-and-removal day for the symptomatic individuals of the 4th cohort and the grouping of the 4th and 5th cohort. On the other hand, Fig. 9b is identical to Fig. 5b, meaning that the 5th cohort's contribution to the dynamics of $\mathcal{R}_0$ is minimal. This is further proved in Fig. 9c and d, where we see that the 2nd cohort dominates the dynamics of the simulation. In particular, when the contact reduction of the 2nd cohort is 50%, scenario $\mathcal{L}$ can be replaced, whereas when the infectious individuals of the 2nd cohort are removed from the community at around the 4th day, scenario $\mathcal{M}$ can be replaced.

(a) $\mathcal{R}_0$ when social distancing is enforced on the 2nd cohort and testing is enforced on the 5th and 6th cohort ($W_\beta = \{2\}$ and $W_\gamma = \{4, 5\}$).

(b) $\mathcal{R}_0$ when social distancing is enforced on the 5th and 6th cohort and testing is enforced on the 2nd cohort ($W_\beta = \{5, 6\}$ and $W_\gamma = \{2\}$).
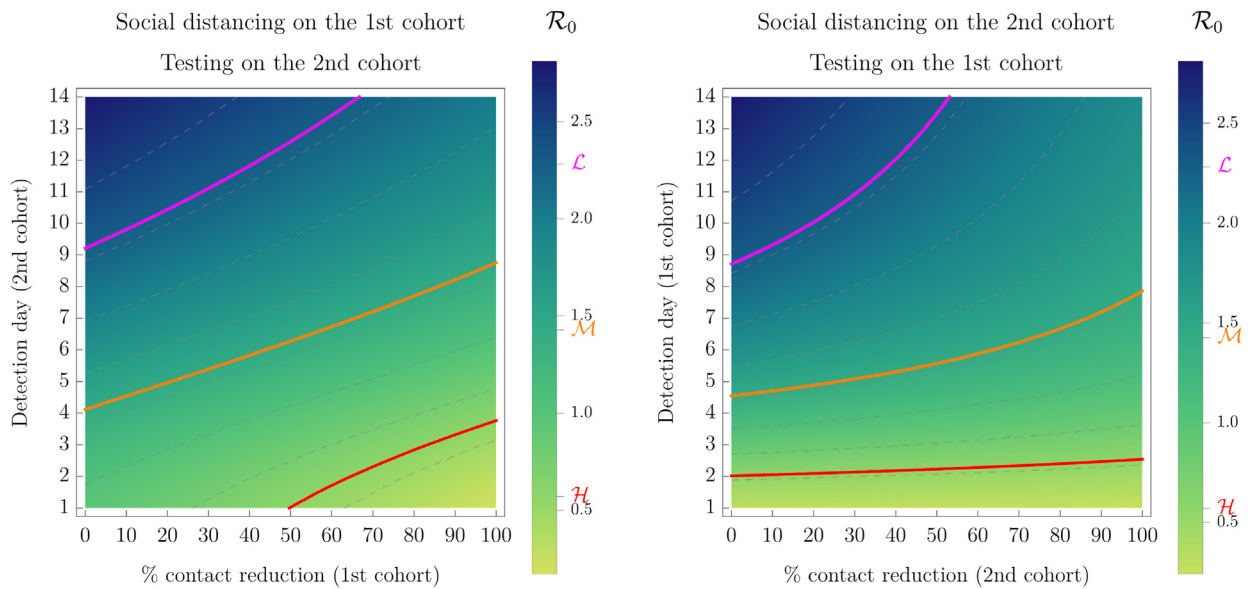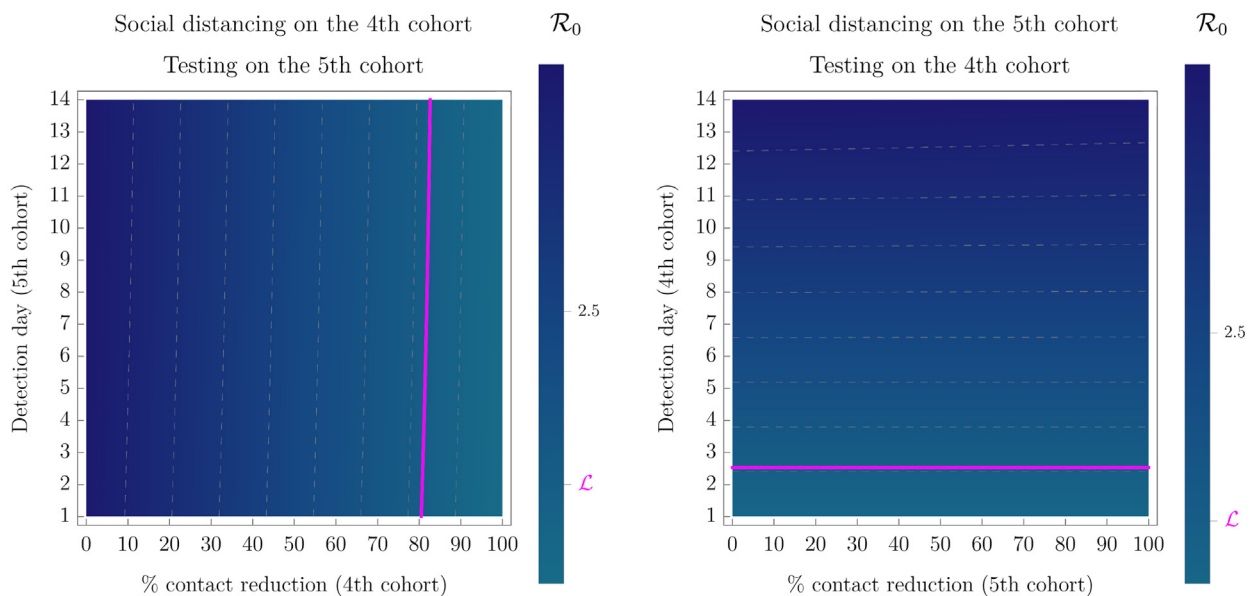
Fig. 5. Two density plots of the 2nd cohort and the grouping of the two older cohorts together. When social distancing is enforced on the 2nd cohort, scenario $\mathcal{H}$ can only be achieved with laxer restriction compared to the respective restrictions on the 1st cohort. Neither of the pictured simulations are able to offer a replacement to scenario $\mathcal{H}$. Much like the simulations of Fig. 3b and Fig. 4b, for the scenario $\mathcal{M}$ to be achieved the testing of the younger cohorts dominates the dynamics of $\mathcal{R}_0$, with the dynamics of the older cohorts being almost irrelevant.
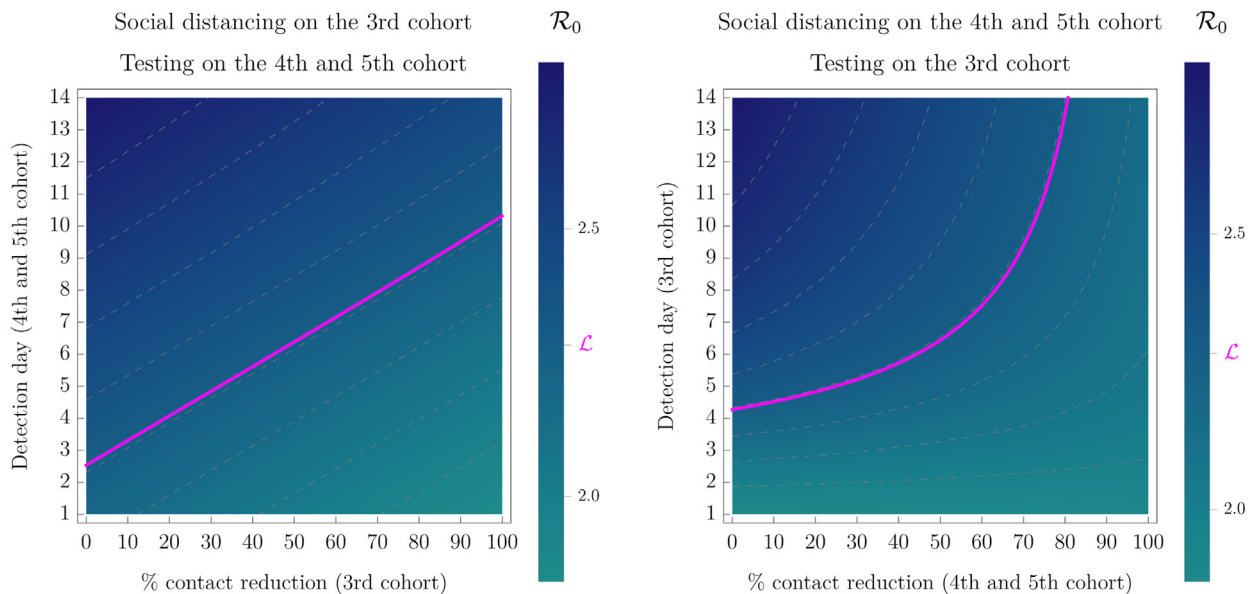
(a) $\mathcal{R}_0$ when social distancing is enforced on the 3rd cohort and testing is enforced on the 5th and 6th cohort ($W_\beta = \{3\}$ and $W_\gamma = \{4, 5\}$).
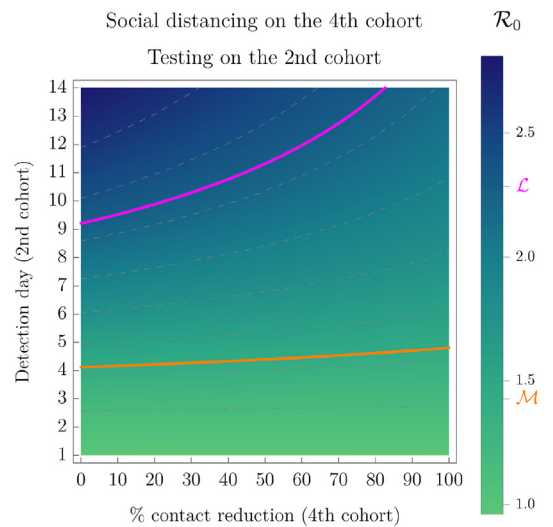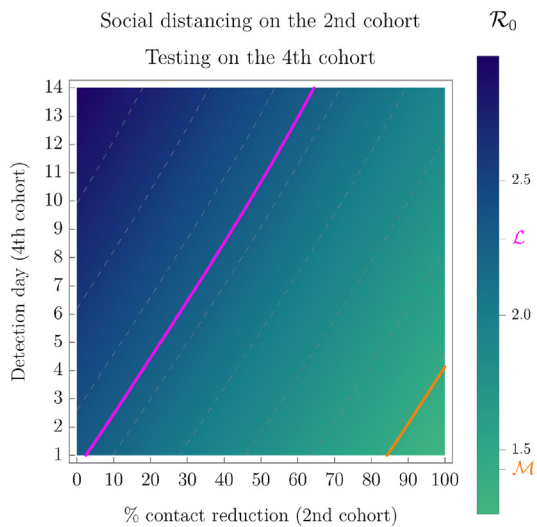
(b) $\mathcal{R}_0$ when social distancing is enforced on the 5th and 6th cohort and testing is enforced on the 3rd cohort ($W_\beta = \{5, 6\}$ and $W_\gamma = \{3\}$).

Fig. 6. Two density plots of the 3rd cohort and the grouping of the two older cohorts together. Neither of the simulations is able to offer a replacement to scenario $\mathcal{M}$ and scenario $\mathcal{H}$. The influence of the 3rd cohort to the dynamics of $\mathcal{R}_0$ is far weaker when compared to the influence of the 1st and 2nd cohort, as can be seen from Fig. 3b and Fig.4b.

Social distancing on the 1st cohort $\mathcal{R}_0$
Testing on the 2nd cohort

Social distancing on the 2nd cohort $\mathcal{R}_0$
Testing on the 1st cohort

(a) $\mathcal{R}_0$ when social distancing is enforced on the 1st cohort and testing is enforced on the 2nd cohort ($W_{\beta} = \{1\}$ and $W_{\gamma} = \{2\}$).

(b) $\mathcal{R}_0$ when social distancing is enforced on the 2nd cohort and testing is enforced on the 1st cohort ($W_{\beta} = \{2\}$ and $W_{\gamma} = \{1\}$).

Fig. 7. Two density plots of the influence of the 1st cohort and 2nd cohort on the dynamics of $\mathcal{R}_0$. In both cases, all three of our horizontal lockdown scenarios $\mathcal{L}, \mathcal{M}$ and $\mathcal{H}$, can be replaced by enforcing a wide range of intensity level restrictions to the 1st cohort and 2nd cohort. The 1st and 2nd cohorts are the most important cohorts at effecting the dynamics of $\mathcal{R}_0$, since they influence the dynamics of $\mathcal{R}_0$ comparably to the influence of the combination of all of our cohorts, as seen in Fig. 4.

Social distancing on the 4th cohort $\mathcal{R}_0$
Testing on the 5th cohort

Social distancing on the 5th cohort $\mathcal{R}_0$
Testing on the 4th cohort

(a) $\mathcal{R}_0$ when social distancing is enforced on the 4th cohort and testing is enforced on the 5th cohort ($W_{\beta} = \{4\}$ and $W_{\gamma} = \{5\}$).
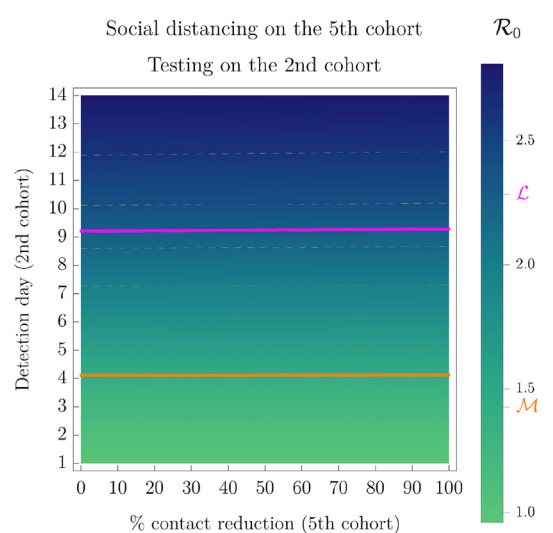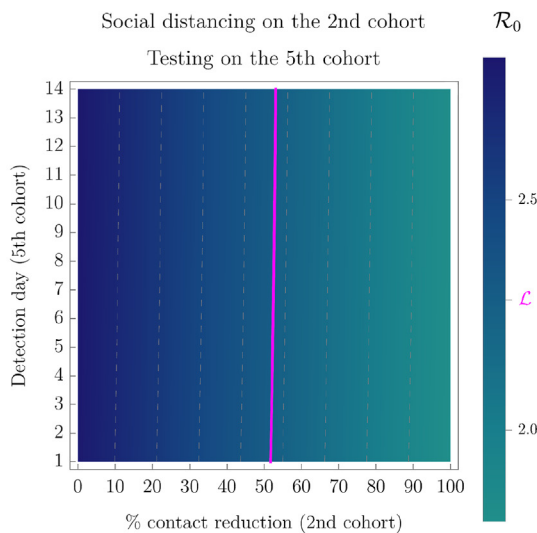
(b) $\mathcal{R}_0$ when social distancing is enforced on the 5th cohort and testing is enforced on the 4th cohort ($W_{\beta} = \{5\}$ and $W_{\gamma} = \{4\}$).

Fig. 8. Two density plots of the influence of the 4th and 5th cohort on the dynamics of $\mathcal{R}_0$. Neither case was able to offer a replacement to horizontal lockdown scenario $\mathcal{M}$ and scenario $\mathcal{H}$. Restrictions on the combination of the 4th cohort and the 5th cohort result in the poorest reduction in $\mathcal{R}_0$ when compared to the remaining of our simulations. When measures are imposed to the 4th and 5th cohort, the restrictions on the 4th cohort dominate the dynamics of $\mathcal{R}_0$.

(a) $\mathcal{R}_0$ when social distancing is enforced on the 2nd cohort and testing is enforced on the 4th cohort ($W_\beta = \{2\}$ and $W_\gamma = \{4\}$).

(b) $\mathcal{R}_0$ when social distancing is enforced on the 4th cohort and testing is enforced on the 2nd cohort ($W_\beta = \{4\}$ and $W_\gamma = \{2\}$).

(c) $\mathcal{R}_0$ when social distancing is enforced on the 2nd cohort and testing is enforced on the 5th cohort ($W_\beta = \{2\}$ and $W_\gamma = \{5\}$).

(d) $\mathcal{R}_0$ when social distancing is enforced on the 5th cohort and testing is enforced on the 2nd cohort ($W_\beta = \{5\}$ and $W_\gamma = \{2\}$).

Fig. 9. Four density plots of the influence of the interactions of the 2nd and 4th cohort, as well as the 2nd and 5th cohort, on the dynamics of $\mathcal{R}_0$. None of the simulations was able to offer a replacement to horizontal lockdown scenario $\mathcal{H}$. The 5th cohort's contribution to the dynamics of $\mathcal{R}_0$ is insignificant, since its removal from the measure-targeted cohorts, minimally affects the dynamics of $\mathcal{R}_0$, as can be seen when Fig. 9a and Fig. 9b and Fig. 5 are compared. Additionally, the 2nd cohort completely dominates the dynamics of $\mathcal{R}_0$, when the 5th cohort is included in the simulations, as can be seen from Fig. 9c and Fig. 9d.

3.4.2. Epidemiological overview of the results, S_1 versus S_2

Throughout our simulations we let (a, b) of each gradation to take values in the 2D interval $[0, 1)^2$ and illustrate the results in contour plots, where in the x-axis and y-axis we have $a \cdot 100\%$ and $b \cdot P_{I \to R} = \frac{b}{\gamma_I} = b \cdot 14$ days, respectively.

$\mathcal{H}$ **versus** S_2. We begin by examining how many substrategies of $\{S_{2_i}\}_{i=1}^{16}$ can be considered as an alternative to scenario $\mathcal{H}$. As can be seen from Fig. 10a, five substrategies of $\{S_{2_i}\}_{i=1}^{16}$ admit the same $\mathcal{R}_0$ as the respective one of scenario $\mathcal{H}$. Therefore, the epidemiological coverage of scenario $\mathcal{H}$ by the substrategies $\{S_{2_i}\}_{i=1}^{16}$ is 31.25%. We highlight the fact that every one of the five substrategies that can replace scenario $\mathcal{M}$, regards restrictions on the 1st cohort.

$\mathcal{M}$ **versus** S_2. Next, we examine how many substrategies of $\{S_{2_i}\}_{i=1}^{16}$ can be considered as an alternative to scenario $\mathcal{M}$. As can be seen from Fig. 10b, eleven substrategies of $\{S_{2_i}\}_{i=1}^{16}$ admit the same $\mathcal{R}_0$ as the respective one of scenario $\mathcal{M}$. Therefore,
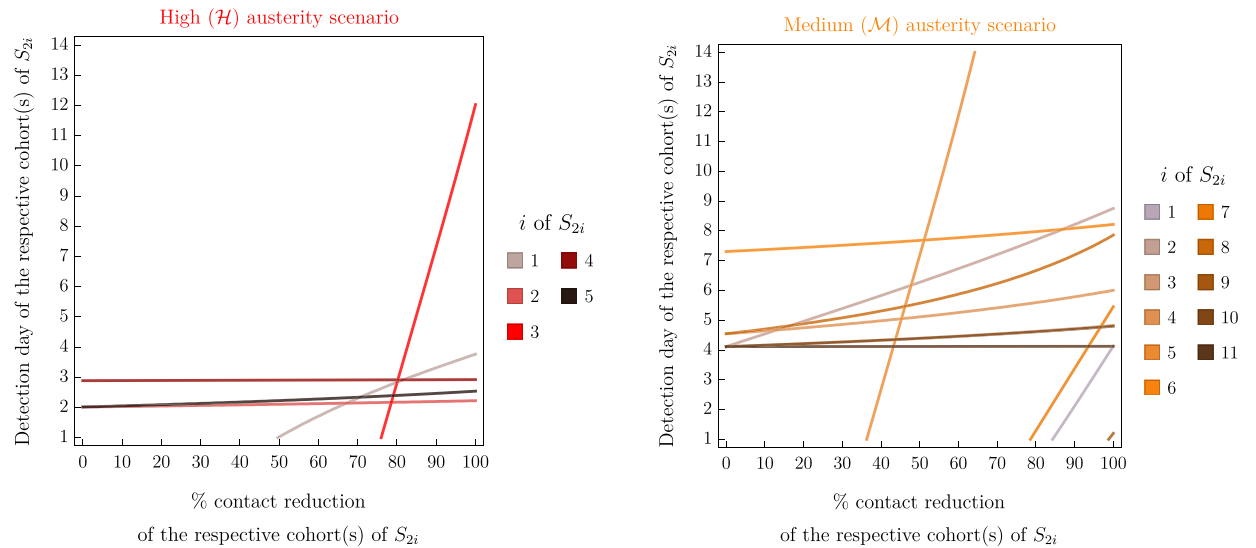
(a) Loci of $\left(a \cdot 100\%, \frac{b}{\gamma_I}\right)$ of the respective substrategies of the family $\{S_{2_i}\}_{i=1}^{16}$ such that their $\mathcal{R}_0$ is equal to 0.571, i.e, the $\mathcal{R}_0$ of scenario $\mathcal{H}$.

(b) Loci of $\left(a \cdot 100\%, \frac{b}{\gamma_I}\right)$ of the respective substrategies of the family $\{S_{2_i}\}_{i=1}^{16}$ such that their $\mathcal{R}_0$ is equal to 1.427, i.e, the $\mathcal{R}_0$ of scenario $\mathcal{M}$.
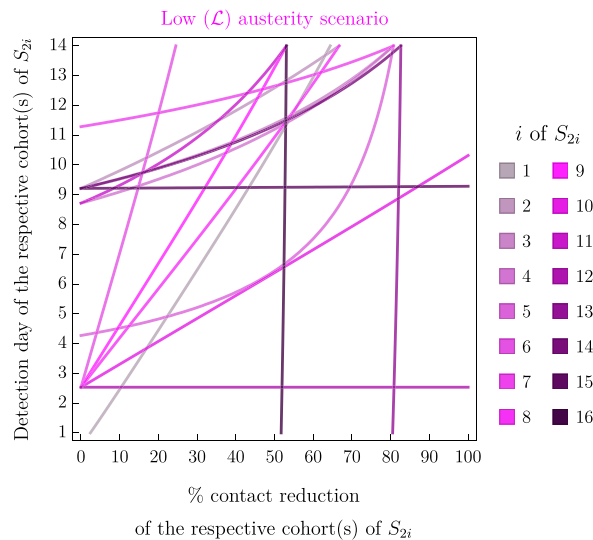
(c) Loci of $\left(a \cdot 100\%, \frac{b}{\gamma_I}\right)$ of the respective substrategies of the family $\{S_{2_i}\}_{i=1}^{16}$ such that their $\mathcal{R}_0$ is equal to 2.283, i.e, the $\mathcal{R}_0$ of scenario $\mathcal{L}$.

Fig. 10. Three contour plots illustrating the epidemiological coverage of each substrategy ($\mathcal{L}$, $\mathcal{M}$ and $\mathcal{H}$) of horizontal lockdown strategy. The denser the plot is, the higher the epidemiological coverage.

Table 5

Horizontal lockdowns versus age-based restrictions. The total coverage of horizontal lockdowns from age-based restrictions is 66.66%. Additionally, the table is populated with representative values of $\left(a \cdot 100\%, \frac{b}{\gamma_I}\right)$ of the strategic scale that each age-based strategy needs to have in order for the strategy to have the same $\mathcal{R}_0$ as each of the three horizontal lockdown scenarios.

Age-based restrictions	Horizontal lockdowns			Epidemiological coverage
	High ($\mathcal{H}$)	Medium ($\mathcal{M}$)	Low ($\mathcal{L}$)	
Contact reduction: 1st, 2nd, 3rd cohorts Testing: 4th, 5th cohorts	80.6% and 3.06 days 88% and 6.4 days 95.4% and 9.82 days	42.3% and 3.71 days 50.5% and 7.43 days 58.9% and 11.4 days	4.55% and 11.7 days 12.5% and 8.19 days 19.9% and 4.59 days	100%
Contact reduction: 4th, 5th cohorts Testing: 1st, 2nd, 3rd cohorts	21.1% and 2.92 days 50.4% and 2.9 days 81.7% and 2.89 days	18.4% and 7.43 days 50% and 7.68 days 78.9% and 7.96 days	17.8% and 13.4 days 42.9% and 12.4 days 67.9% and 11.7 days	100%
Contact reduction: 1st cohort Testing: 4th, 5th cohorts	✗	98.8% and 1 day 99.1% and 1.05 days 99.5% and 1.12 days	10.7% and 11.9 days 34% and 8.18 days 55.4% and 4.31 days	66.66%
Contact reduction: 4th, 5th cohorts Testing: 1st cohort	18.8% and 2.05 days 48.6% and 2.1 days 80.2% and 2.18 days	17.9% and 4.72 days 50% and 5.11 days 79.1% and 5.57 days	17.5% and 9.41 days 43.2% and 10.8 days 68.6% and 12.7 days	100%
Contact reduction: 2nd cohort Testing: 4th, 5th cohorts	✗	82.7% and 1.86 days 89.6% and 3.29 days 96.4% and 4.71 days	10.6% and 11.7 days 27.7% and 8.32 days 43% and 4.73 days	66.66%
Contact reduction: 4th, 5th cohorts Testing: 2nd cohort	✗	21.2% and 4.65 days 50% and 4.4 days 82.1% and 4.22 days	17.9% and 9.82 days 43.1% and 11 days 67.9% and 12.7 days	66.66%
Contact reduction: 3rd cohort Testing: 4th, 5th cohorts	✗	✗	19.5% and 8.89 days 50.9% and 6.45 days 82.1% and 4.04 days	33.33%
Contact reduction: 4th, 5th cohorts Testing: 3rd cohort	✗	✗	23.1% and 4.93 days 54.7% and 6.89 days 75% and 11 days	33.33%
Contact reduction: 1st cohort Testing: 2nd cohort	58.1% and 3.29 days 74% and 2.52 days 89.5% and 1.59 days	19.6% and 4.95 days 50% and 6.27 days 80.2% and 7.71 days	14% and 10.1 days 34.3% and 11.4 days 54.5% and 13 days	100%
Contact reduction: 2nd cohort Testing: 1st cohort	20.2% and 2.41 days 51.2% and 2.23 days 82% and 2.09 days	20.1% and 4.88 days 52.5% and 5.64 days 82.1% and 6.77 days	10.7% and 9.36 days 28.2% and 10.8 days 44.4% and 12.6 days	100%
Contact reduction: 4th cohort Testing: 5th cohort	✗	✗	81.1% and 3.46 days 81.8% and 7.5 days 82.3% and 11.2 days	33.33%
Contact reduction: 5th cohort Testing: 4th cohort	✗	✗	18.9% and 2.53 days 48.9% and 2.53 days 79.7% and 2.53 days	33.33%
Contact reduction: 2nd cohort Testing: 4th cohort	✗	87.5% and 1.62 days 92% and 2.51 days 96.4% and 3.41 days	11.5% and 2.76 days 33.8% and 7.25 days 52.8% and 11.3 days	66.66%
Contact reduction: 4th cohort Testing: 2nd cohort	✗	21.4% and 4.63 days 51.1% and 4.4 days 81.5% and 4.22 days	17.9% and 9.81 days 44.5% and 11 days 68.1% and 12.6 days	66.66%
Contact reduction: 2nd cohort Testing: 5th cohort	✗	✗	52.1% and 3.52 days 52.5% and 7.36 days 52.9% and 11.3 days	33.33%
Contact reduction: 5th cohort Testing: 2nd cohort	✗	20.4% and 4.12 days 51% and 4.12 days 81.2% and 4.12 days	18.9% and 9.22 days 49.1% and 9.25 days 79.3% and 9.27 day	66.66%
Social coverage	31.25%	68.75%	100%	66.66%

the epidemiological coverage of scenario $\mathcal{M}$ by the substrategies $\{S_{2_i}\}_{i=1}^{16}$ is 68.75%. We highlight the fact that every one of the eleven substrategies that can replace scenario $\mathcal{M}$, regards restrictions on the 1st and 2nd cohort.

$\mathcal{L}$ **versus S_2**. Finally, we examine how many substrategies of $\{S_{2_i}\}_{i=1}^{16}$ can be considered as an alternative to scenario $\mathcal{L}$. As can be seen from Fig. 10c, all substrategies $\{S_{2_i}\}_{i=1}^{16}$ admit the same $\mathcal{R}_0$ as the respective one of scenario $\mathcal{L}$. Therefore, the epidemiological coverage of scenario $\mathcal{L}$ by the substrategies $\{S_{2_i}\}_{i=1}^{16}$ is 100%.

A summary of the results of §3 can be seen in Table 5.

4. Conclusions and discussion

In this paper, we introduced a scheme for the comparison of certain types of interventions for the restriction of an epidemiological phenomenon. This scheme incorporates some novel notions such as "strategy", "substrategy", "gradable strategy" and its "gradation", "comparison table", as well as "epidemiological coverage" and "social coverage". Then, we utilized the aforementioned scheme and the age-based epidemiological compartment problem studied in Bitsouni et al. (2024) to compare horizontal lockdown policies with various age-based interventions.

In particular, we distributed the total population into five cohorts, based on the age of each individual (in ascending order) and we defined the graded strategy of horizontal lockdowns, considering three scenarios of horizontal lockdowns with varying intensity, Low ($\mathcal{L}$), Medium ($\mathcal{M}$) and High ($\mathcal{H}$). We also defined the strategy of age-based restrictions, consisting of 16 substrategies. In general, our results suggest that these two strategies are comparable mainly at low or medium level of intensity. Particularly, throughout our simulations, which used data from the literature, we deduced that the strategies that targeted the 1st and 2nd cohort had the best epidemiological coverage. Moreover, all substrategies were able to admit the same $\mathcal{R}_0$ as the respective one of scenario $\mathcal{L}$, meaning a 100% social coverage of $\mathcal{L}$, while the social coverage of scenarios $\mathcal{M}$ and $\mathcal{H}$ by the substrategies is 68.75% and 31.25%, respectively.

Future work could entail the generalization of the notion of strategy, hence the comparison process itself.

CRediT authorship contribution statement

Vasiliki Bitsouni: Writing − original draft, Conceptualization. **Nikolaos Gialelis:** Writing − original draft, Conceptualization. **Vasilis Tsilidis:** Writing − original draft, Conceptualization.

Declaration of competing interest

The authors declare that they have no known competing financial interests or personal relationships that could have appeared to influence the work reported in this paper.

Acknowledgment

Appendix A. The employed epidemiological model

Here we use the epidemiological model $\mathcal{M}$ along with the respective problem $\mathcal{P}$, introduced and studied in Bitsouni et al. (2024), as a means of utilization of the proposed scheme in answering the main question of the present paper. We choose this model as it incorporates both symptomatic and asymptomatic infectious individuals, with the latter playing an important role in the spread of the COVID-19 (see Gao et al. (2021) and many references therein), as well as the age of the infected/infectious individuals.

After *scaling* the independent age-variable, θ, and turning it to another time-variable measured in the same units as t (see Bitsouni et al. (2024)) and using the relation $N = S + V + E + A + I + R$, we obtain the following model

$$\begin{cases} \dfrac{\mathrm{d}S}{\mathrm{d}t} = \mu N_0 - \left(p + \int\limits_0^\infty \beta_A(\theta)a(\,\cdot\,,\theta) + \beta_I(\theta)i(\,\cdot\,,\theta)\,\mathrm{d}\theta + \mu \right)S \\ S(0) = S_0, \end{cases} \tag{4a}$$

$$\begin{cases} \dfrac{\mathrm{d}V}{\mathrm{d}t} = pS - \left(\zeta\epsilon + \int\limits_0^\infty \beta_A(\theta)a(\,\cdot\,,\theta) + \beta_I(\theta)i(\,\cdot\,,\theta)\,\mathrm{d}\theta(1-\epsilon) + \mu \right)V \\ V(0) = V_0, \end{cases} \tag{4b}$$

$$\begin{cases} \dfrac{\partial e}{\partial t} + \dfrac{\partial e}{\partial \theta} = -(k+\mu)e \\ e(\,\cdot\,,0) = \int\limits_0^\infty \beta_A(\theta)a(\,\cdot\,,\theta) + \beta_I(\theta)i(\,\cdot\,,\theta)\,\mathrm{d}\theta(S+(1-\epsilon)V) \\ e(0,\,\cdot\,) = e_0, \end{cases} \tag{4c}$$

$$
\begin{cases}
\dfrac{\partial a}{\partial t} + \dfrac{\partial a}{\partial \theta} = -(\gamma_A \xi + \chi(1-\xi) + \mu)a \\[2mm]
a(\cdot, 0) = \displaystyle\int_0^\infty k(\theta)q(\theta)e(\cdot, \theta)\,\mathrm{d}\theta \\[2mm]
a(0, \cdot) = a_0,
\end{cases}
\tag{4d}
$$

$$
\begin{cases}
\dfrac{\partial i}{\partial t} + \dfrac{\partial i}{\partial \theta} = -(\gamma_I + \mu)i \\[2mm]
i(\cdot, 0) = \displaystyle\int_0^\infty k(\theta)(1-q(\theta))e(\cdot, \theta) + \chi(\theta)(1-\xi(\theta))a(\cdot, \theta)\,\mathrm{d}\theta \\[2mm]
i(0, \cdot) = i_0.
\end{cases}
\tag{4e}
$$

The flow diagram of the differential equations in (4) is shown in Fig. 11, and the dimensional units of all variables and parameters appeared in $\mathscr{P}$ (4) are gathered in Table 6.
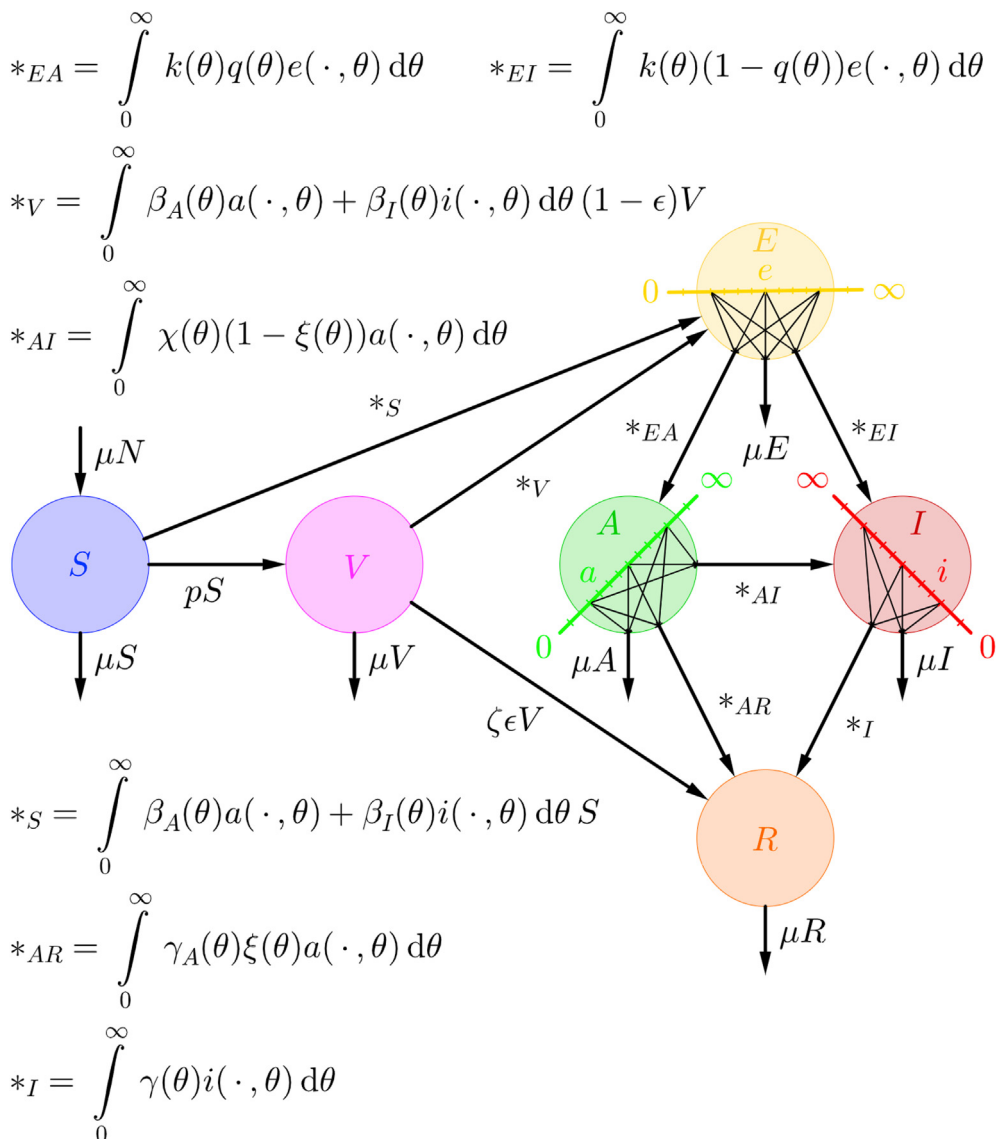
Fig. 11. Flow diagram of $\mathscr{P}$ (4).

Table 6
Description of the independent and dependent variables and parameters of $\mathscr{M}$, along with their units.

Independent variables	Description	Units
t	Time	T
θ	Age, i.e., time elapsed since, e.g., birth or infection	Θ

Conversion factor	Description	Units
ω	Conversion factor from the units of θ to the units of t	$T\,\Theta^{-1}$

Dependent variables	Description	Units
N	Number of total population of individuals	#
S	Number of susceptible individuals	#
V	Number of vaccinated-with-a-prophylactic-vaccine individuals	#
e	Age density of latent/exposed individuals	$\#\,\Theta^{-1}$
E	Number of latent/exposed individuals	#
a	Age density of asymptomatic infectious individuals	$\#\,\Theta^{-1}$
A	Number of asymptomatic infectious individuals	#
i	Age density of symptomatic infectious	$\#\,\Theta^{-1}$
I	Number of symptomatic infectious individuals	#
R	Number of recovered/removed individuals	#

Parameters	Description	Units
N_0	Population size	#
μ	Birth/Death rate	T^{-1}
β_A	Transmission rate of asymptomatic infectious individuals	$\#^{-1}\,T^{-1}$
β_I	Transmission rate of symptomatic infectious individuals	$\#^{-1}\,T^{-1}$
p	Vaccination rate	T^{-1}
ϵ	Vaccine effectiveness	—
ζ	Vaccine-induced immunity rate	T^{-1}
k	Latent rate (rate of susceptible individuals becoming infectious)	T^{-1}
q	Proportion of the latent/exposed individuals becoming asymptomatic infectious	—
ξ	Proportion of the asymptomatic infectious individuals becoming recovered/removed (without developing any symptoms)	—
χ	Incubation rate (rate of a part of asymptomatic infectious individuals developing symptoms)	T^{-1}
γ_A	Recovery rate of asymptomatic infectious individuals	T^{-1}
γ_I	Recovery rate of symptomatic infectious individuals	T^{-1}

From the analysis conducted in Bitsouni et al. (2024), the *basic reproductive number*, $\mathcal{R}_0$, of the model is

$$\mathbb{R}_0^+ \ni \mathcal{R}_0 := \frac{\mu N_0}{p+\mu}\left(1+\frac{p(1-\epsilon)}{\zeta\epsilon+\mu}\right)(\mathcal{R}_A+\mathcal{R}_I), \tag{5}$$

where

$$\mathbb{R}_0^+ \ni \mathcal{R}_A := \int_0^\infty k(s)q(s)\mathrm{e}^{-\int_0^s k(\tau)+\mu\,\mathrm{d}\tau}\,\mathrm{d}s\int_0^\infty \beta_A(s)\mathrm{e}^{-\int_0^s \gamma_A(\tau)\xi(\tau)+\chi(\tau)(1-\xi(\tau))+\mu\,\mathrm{d}\tau}\,\mathrm{d}s$$

and

$$\mathbb{R}_0^+ \ni \mathcal{R}_I := \left(\begin{array}{l} \displaystyle\int_0^\infty k(s)(1-q(s))\mathrm{e}^{-\int_0^s k(\tau)+\mu\,\mathrm{d}\tau}\,\mathrm{d}s+ \\[1.5em] +\displaystyle\int_0^\infty k(s)q(s)\mathrm{e}^{-\int_0^s k(\tau)+\mu\,\mathrm{d}\tau}\,\mathrm{d}s\int_0^\infty \chi(s)(1-\xi(s))\mathrm{e}^{-\int_0^s \gamma_A(\tau)\xi(\tau)+\chi(\tau)(1-\xi(\tau))+\mu\,\mathrm{d}\tau}\,\mathrm{d}s \end{array}\right)\times\int_0^\infty \beta_I(s)\mathrm{e}^{-\int_0^s \gamma_I(\tau)+\mu\,\mathrm{d}\tau}\,\mathrm{d}s.$$

Appendix B. Parameter estimation

We now present parameter values fitting for the case of SARS-CoV-2. The chosen values are taken from the biological and medical literature. Bellow, we give a detailed explanation about the value of each parameter, whereas a summary of the parameter values can be found in Table 1.

The size of the population, $N_0 = 80 \cdot 10^6$ individuals, is assumed to be that of a relative large country, such as Germany, Turkey, or Thailand (Mathieu et al., 2020).

The birth/death rate, $\mu = 4.38356 \cdot 10^{-5}$ day^{-1}, is taken from data from Mathieu et al. (2020). The average birth/death rate of the world for the year 2021 is about 16 per 1000 individuals per year. Hence, we convert the aforementioned quantity from "per 1000 individuals per year" to "per day" to get

$$16 \frac{1}{1000 \text{ individuals} \cdot \text{year}} \mapsto 16 \cdot 10^{-3} \frac{1}{365 \text{ days}} = 4.38356 \cdot 10^{-5} \text{ day}^{-1} = \mu.$$

For the transmission rate of asymptomatic and symptomatic infectious individuals, we firstly assume the probability of an exposed individual passing to the compartments of asymptomatic and symptomatic individuals to be $\varpi_{E \to A} = \frac{1}{8}$ and $\varpi_{E \to I} = \frac{1}{3}$, respectively. From Del Valle et al. (2007), we have that the average number of daily contacts of any person, regardless its epidemiological status, of age θ, $c(\theta)$, follows the graph as seen in Fig. 12. To digitize the data of the contacts, we use Web-PlotDigitizer 4.6 (Rohatgi, 2022) to manually extract data points from Fig. 2 of Del Valle et al. (2007) and then interpolated them using a third order polynomial interpolation scheme through Mathematica 13.1 (Wolfram Research Inc., 2022) and the function Interpolation. Subsequently, from (1) we deduce that the transmission rate of asymptomatic and symptomatic infectious individuals are the functions presented in Fig. 13.
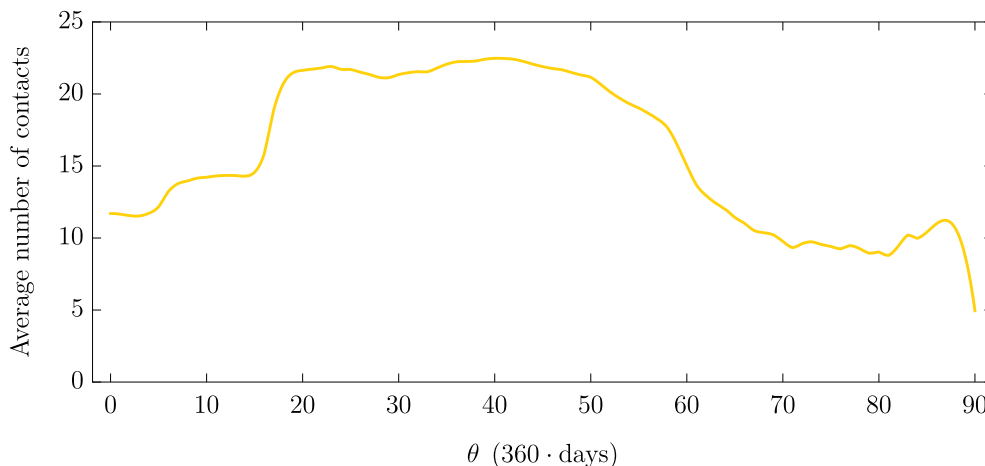

Fig. 12. Age density (in years) of the average number of daily contacts, c, taken from Del Valle et al. (2007).
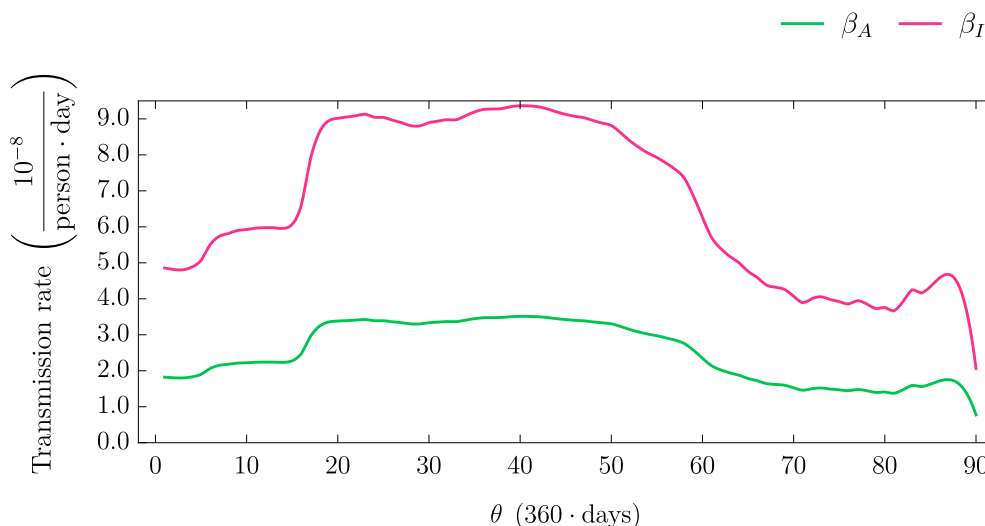

Fig. 13. Estimation of the age density (in years) of the asymptomatic and symptomatic transmission rate, assuming $\beta_A = \frac{c_A \cdot \varpi_{E \to A}}{N_0}$ and $\beta_I = \frac{c_I \cdot \varpi_{E \to I}}{N_0}$ according to (1), where $c_A = c = c_I$.

The vaccination rate, $p = 10^{-3}$ day^{-1}, is taken from data from Mathieu et al. (2020), during the summer of 2021 in the USA, when the Delta variant of SARS-CoV-2 was the dominant variant. During the end of summer, the percentage of fully vaccinated USA citizens was about 54% whereas in the beginning of summer it was around 45%. Hence, we estimate the vaccination from that three-month period to be $p = \frac{54\% - 45\%}{90}$ day$^{-1} = 10^{-3}$ day^{-1}.

The vaccine effectiveness, $\epsilon = 0.7$, is estimated from data from Grant et al. (2022). In Grant et al. (2022), the authors find that with the BNT162b2 vaccine, the effectiveness of two doses is 88.0% among those with the Delta variant, whereas with the ChAdOx1 nCoV-19 vaccine, the respective effectiveness of two doses was 67.0%. Hence, we assume $\epsilon = 0.7$.

The vaccine-induced immunity rate, $\zeta = \frac{1}{14}$ day^{-1}, is estimated from data from Chau et al. (2022). The authors of Chau et al. (2022) report that, after two weeks of the second dose of the ChAdOx1 nCoV-19 vaccine, the percentage of study participants with detectable neutralizing antibodies reached 98.1%.

The latent rate, k, is found by estimating that the latent and incubation period differ by 1 day. In Kang et al. (2022), the authors examined data from 93 Delta transmission pairs and estimated the latent period by fitting the data to the Weibull distribution, which made the best fit. They found the mean latent period to be 3.9 days. In Wu et al. (2022), the authors performed a systematic review and meta-analysis of 141 articles and found that the incubation periods of COVID-19 caused by the Alpha, Beta, Delta, and Omicron variants were 5.00, 4.50, 4.41, and 3.42 days, respectively. Hence, assuming that the latent and incubation period vary by 1 day, we have that $k = \frac{\chi}{1-\chi}$, and by substituting χ as found later in the present section, we have that

$$
k(\theta) = \begin{cases}
\frac{1}{4} \text{ day}^{-1}, & \theta < 30 \cdot 360 \text{ day} \\
\frac{1}{4.8} \text{ day}^{-1}, & 30 \cdot 360 \text{ day} \leq \theta < 40 \cdot 360 \text{ day} \\
\frac{1}{4.8} \text{ day}^{-1}, & 40 \cdot 360 \text{ day} \leq \theta < 50 \cdot 360 \text{ day} \\
\frac{1}{5.5} \text{ day}^{-1}, & 50 \cdot 360 \text{ day} \leq \theta < 60 \cdot 360 \text{ day} \\
\frac{1}{3.1} \text{ day}^{-1}, & 60 \cdot 360 \text{ day} \leq \theta < 70 \cdot 360 \text{ day} \\
\frac{1}{6} \text{ day}^{-1}, & 70 \cdot 360 \text{ day} \leq \theta,
\end{cases}
\tag{6}
$$

where θ is measured in years.

The proportion of the latent/exposed individuals becoming asymptomatic infectious, q, is taken from Sah et al. (2021), where the authors estimated the asymptomatic proportion by age, by performing a systematic review and meta-analysis of 38 studies involving 14850 individuals. The curve they estimated can be seen in Fig. 14. To digitize the data, we use the same procedure we used for the age density of daily contacts described earlier in the present section.
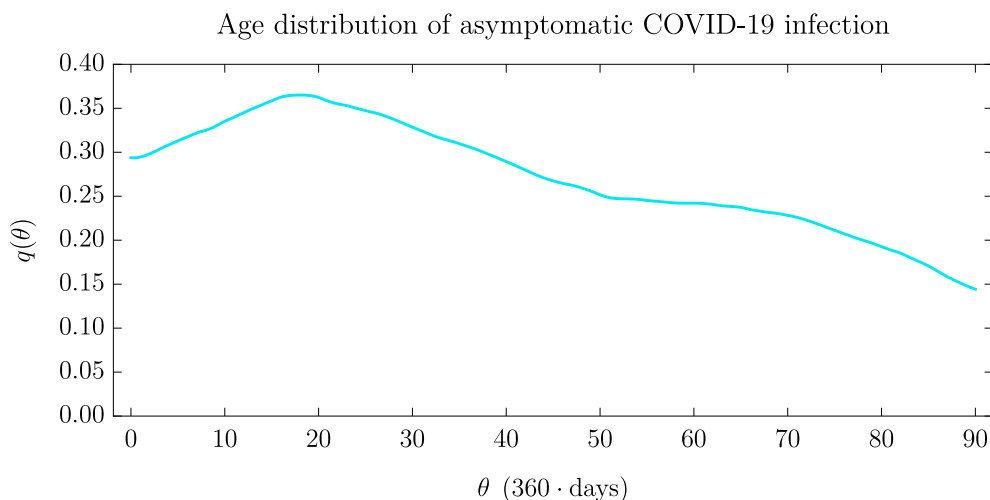

Fig. 14. Percentage of asymptomatic COVID-19 infection, by age (in years), taken from Sah et al. (2021).

The proportion of the asymptomatic infectious individuals becoming recovered/removed without developing any symptoms, $\xi = 0.5$, is estimated from data from He et al. (2021) and Buitrago-Garcia et al. (2022). In He et al. (2021), the

authors performed a systematic review and meta-analysis from 41 studies containing the rate of asymptomatic COVID-19 infection before May 20, 2020, aggregating 50155 patients, and found that nearly half of the patients with no symptoms at the time of their detection, would develop symptoms later. In Buitrago-Garcia et al. (2022), the authors performed a systematic review and meta-analysis from 130 studies and reported the percentage of persistently asymptomatic individuals being between 14 and 50%. Hence, we choose the proportion of persistently asymptomatic individuals being 50%.

The incubation rate, χ, is estimated from data from Tan et al. (2020). The authors of Tan et al. (2020) found that the incubation period varies with age, based on data from Singaporean hospitals between January 23, 2020 and April 2, 2020. The authors divided the participants based on their age (in years) to six groups ($< 30, 30-39, 40-49, 50-59, 60-69$ and $70 <$) and presented their results through a box plot. Hence, we assume that χ is a piecewise function with its domain intervals being the six aforementioned age groups, and with the function being constant on each interval and equal to one over the median of the respective age group. Therefore, we have that

$$\chi(\theta) = \begin{cases} \frac{1}{5} \text{ day}^{-1}, & \theta < 30 \cdot 360 \text{ day} \\ \frac{1}{5.8} \text{ day}^{-1}, & 30 \cdot 360 \text{ day} \leq \theta < 40 \cdot 360 \text{ day} \\ \frac{1}{5.8} \text{ day}^{-1}, & 40 \cdot 360 \text{ day} \leq \theta < 50 \cdot 360 \text{ day} \\ \frac{1}{6.5} \text{ day}^{-1}, & 50 \cdot 360 \text{ day} \leq \theta < 60 \cdot 360 \text{ day} \\ \frac{1}{4.1} \text{ day}^{-1}, & 60 \cdot 360 \text{ day} \leq \theta < 70 \cdot 360 \text{ day} \\ \frac{1}{7} \text{ day}^{-1}, & 70 \cdot 360 \text{ day} \leq \theta, \end{cases} \tag{7}$$

where θ is measured in years.

The recovery rate of asymptomatic infectious individuals, $\gamma_A = \frac{1}{8} \text{ day}^{-1}$, and recovery rate of the symptomatic infectious individuals, $\gamma_I = \frac{1}{14} \text{ day}^{-1}$, is estimated from Byrne et al. (2020). In Byrne et al. (2020), the authors performed a rapid scoping review up to April 1, 2020 and found that the median infectious period for asymptomatic cases was 6.5–9.5 days, whereas time from symptom onset to two negative RT-PCR tests ranged from 10.9 to 15.8 days. Hence, we assume that the recovery period of asymptomatic and symptomatic infectious individuals to be 8 and 14 days respectively.

References

Abell, I. R., McCaw, J. M., & Baker, C. M. (2023). Understanding the impact of disease and vaccine mechanisms on the importance of optimal vaccine allocation. *Infectious Disease Modelling, 8,* 539–550. https://doi.org/10.1016/j.idm.2023.05.003

Acemoglu, D., Chernozhukov, V., Werning, I., & Whinston, M. D. (2021). Optimal targeted lockdowns in a multigroup sir model. *The American Economic Review: Insights, 3,* 487–502. https://doi.org/10.1257/aeri.20200590

Adegbite, G., Edeki, S., Isewon, I., Emmanuel, J., Dokunmu, T., Rotimi, S., Oyelade, J., & Adebiyi, E. (2023). Mathematical modeling of malaria transmission dynamics in humans with mobility and control states. *Infectious Disease Modelling, 8,* 1015–1031. https://doi.org/10.1016/j.idm.2023.08.005

Ahammed, T., Anjum, A., Rahman, M. M., Haider, N., Kock, R., & Uddin, M. J. (2021). Estimation of novel coronavirus (COVID-19) reproduction number and case fatality rate: A systematic review and meta-analysis. *Health Science Reports, 4,* e274. https://doi.org/10.1002/hsr2.274

Amaku, M., Covas, D. T., Coutinho, F. A. B., Neto, R. S. A., Struchiner, C., Wilder-Smith, A., & Massad, E. (2021). Modelling the test, trace and quarantine strategy to control the COVID-19 epidemic in the state of São Paulo, Brazil. *Infectious Disease Modelling, 6,* 46–55. https://doi.org/10.1016/j.idm.2020.11.004

Anupong, S., Chantanasaro, T., Wilasang, C., Jitsuk, N. C., Sararat, C., Sornbundit, K., Pattanasiri, B., Wannigama, D. L., Amarasiri, M., Chadsuthi, S., & Modchang, C. (2023). Modeling vaccination strategies with limited early COVID-19 vaccine access in low-and middle-income countries: A case study of Thailand. *Infectious Disease Modelling, 8,* 1177–1189. https://doi.org/10.1016/j.idm.2023.11.003

Apenteng, O. O., Osei, P. P., Oduro, B., Kwabla, M. P., & Ismail, N. A. (2020). The impact of implementing HIV prevention policies therapy and control strategy among HIV and AIDS incidence cases in Malaysia. *Infectious Disease Modelling, 5,* 755–765. https://doi.org/10.1016/j.idm.2020.09.009

Asahi, K., Undurraga, E. A., Valdés, R., & Wagner, R. (2021). The effect of COVID-19 on the economy: Evidence from an early adopter of localized lockdowns. *Journal of Global Health, 11.* https://doi.org/10.7189/jogh.10.05002

Béraud, G., Timsit, J.-F., & Leleu, H. (2022). Remdesivir and dexamethasone as tools to relieve hospital care systems stressed by COVID-19: A modelling study on bed resources and budget impact. *PLoS One, 17,* Article e0262462. https://doi.org/10.1371/journal.pone.0262462

Bhadauria, A. S., Dhungana, H. N., Verma, V., Woodcock, S., & Rai, T. (2023). Studying the efficacy of isolation as a control strategy and elimination of tuberculosis in India: A mathematical model. *Infectious Disease Modelling, 8,* 458–470. https://doi.org/10.1016/j.idm.2023.03.005

Billah, M. A., Miah, M. M., & Khan, M. N. (2020). Reproductive number of coronavirus: A systematic review and meta-analysis based on global level evidence. *PLoS One, 15,* Article e0242128. https://doi.org/10.1371/journal.pone.0242128

Bitsouni, V., Gialelis, N., & Tsilidis, V. (2024). An age-structured SVEAIR epidemiological model. *Mathematical Methods in the Applied Sciences.* https://doi.org/10.1002/mma.10165

Brethouwer, J.-T., van de Rijt, A., Lindelauf, R., & Fokkink, R. (2021). "Stay nearby or get checked": A covid-19 control strategy. *Infectious Disease Modelling, 6,* 36–45. https://doi.org/10.1016/j.idm.2020.10.013

Brodeur, A., Gray, D., Islam, A., & Bhuiyan, S. (2021). A literature review of the economics of COVID-19. *Journal of Economic Surveys, 35,* 1007–1044. https://doi.org/10.1111/joes.12423

Buitrago-Garcia, D., Ipekci, A. M., Heron, L., Imeri, H., Araujo-Chaveron, L., Arevalo-Rodriguez, I., Ciapponi, A., Cevik, M., Hauser, A., Alam, M. I., et al. (2022). Occurrence and transmission potential of asymptomatic and presymptomatic SARS-CoV-2 infections: Update of a living systematic review and meta-analysis. *PLoS Medicine, 19*, Article e1003987. https://doi.org/10.1371/journal.pmed.1003987

Byrne, A. W., McEvoy, D., Collins, A. B., Hunt, K., Casey, M., Barber, A., Butler, F., Griffin, J., Lane, E. A., McAloon, C., et al. (2020). Inferred duration of infectious period of SARS-CoV-2: Rapid scoping review and analysis of available evidence for asymptomatic and symptomatic COVID-19 cases. *BMJ Open, 10*, Article e039856. https://doi.org/10.1136/bmjopen-2020-039856

Centers for disease control and prevention. URL: https://www.cdc.gov/coronavirus/2019-ncov/hcp/testing-overview.html, (2020).

Chau, N. V. V., Nguyet, L. A., Truong, N. T., Dung, N. T., Nhan, M. T., Man, D. N. H., Ngoc, N. M., Thao, H. P., Tu, T. N. H., Mai, H. K., et al. (2022). Immunogenicity of Oxford-AstraZeneca COVID-19 vaccine in Vietnamese health-care workers. *The American Journal of Tropical Medicine and Hygiene, 106*, 556. https://doi.org/10.4269/ajtmh.21-0849

Chen, J., Vullikanti, A., Santos, J., Venkatramanan, S., Hoops, S., Mortveit, H., Lewis, B., You, W., Eubank, S., Marathe, M., et al. (2021). Epidemiological and economic impact of COVID-19 in the US. *Scientific Reports, 11*, Article 20451. https://doi.org/10.1038/s41598-021-99712-z

Deb, P., Furceri, D., Ostry, J. D., & Tawk, N. (2021). The economic effects of COVID-19 containment measures. *Open Economies Review, 33*, 1–32. https://doi.org/10.1007/s11079-021-09638-2

Del Valle, S., Hyman, J., Hethcote, H., & Eubank, S. (2007). Mixing patterns between age groups in social networks. *Social Networks, 29*, 539–554. https://doi.org/10.1016/j.socnet.2007.04.005

Demers, J., Fagan, W. F., Potluri, S., & Calabrese, J. M. (2023). The relationship between controllability, optimal testing resource allocation, and incubation-latent period mismatch as revealed by COVID-19. *Infectious Disease Modelling, 8*, 514–538. https://doi.org/10.1016/j.idm.2023.04.007

Diekmann, O., & Heesterbeek, J. A. P. (2000). *Mathematical epidemiology of infectious diseases: Model building, analysis and interpretation, ume 5*. John Wiley & Sons.

Gan, G., Janhavi, A., Tong, G., Lim, J. T., & Dickens, B. L. (2024). The need for pre-emptive control strategies for mpox in Asia and Oceania. *Infectious Disease Modelling, 9*, 214–223. https://doi.org/10.1016/j.idm.2023.12.005

Gao, Z., Xu, Y., Sun, C., Wang, X., Guo, Y., Qiu, S., & Ma, K. (2021). A systematic review of asymptomatic infections with COVID-19. *Journal of Microbiology, Immunology, and Infection, 54*, 12–16. https://doi.org/10.1016/j.jmii.2020.05.001

Grant, R., Charmet, T., Schaeffer, L., Galmiche, S., Madec, Y., Von Platen, C., Chény, O., Omar, F., David, C., Rogoff, A., et al. (2022). Impact of SARS-CoV-2 Delta variant on incubation, transmission settings and vaccine effectiveness: Results from a nationwide case-control study in France. *The Lancet Regional Health - Europe, 13*, Article 100278. https://doi.org/10.1016/j.lanepe.2021.100278

He, J., Guo, Y., Mao, R., & Zhang, J. (2021). Proportion of asymptomatic coronavirus disease 2019: A systematic review and meta-analysis. *Journal of Medical Virology, 93*, 820–830. https://doi.org/10.1002/jmv.26326

Kang, M., Xin, H., Yuan, J., Ali, S. T., Liang, Z., Zhang, J., Hu, T., Lau, E. H., Zhang, Y., Zhang, M., et al. (2022). Transmission dynamics and epidemiological characteristics of SARS-CoV-2 Delta variant infections in Guangdong, China, May to June 2021. *Euro Surveillance, 27*, Article 2100815. https://doi.org/10.2807/1560-7917.ES.2022.27.10.2100815

Karatayev, V. A., Anand, M., & Bauch, C. T. (2020). Local lockdowns outperform global lockdown on the far side of the COVID-19 epidemic curve. *Proceedings of the National Academy of Sciences, 117*, 24575–24580. https://doi.org/10.1073/pnas.2014385117

Kirwin, E., Rafferty, E., Harback, K., Round, J., & McCabe, C. (2021). A net benefit approach for the optimal allocation of a covid-19 vaccine. *PharmacoEconomics, 39*, 1059–1073. https://doi.org/10.1007/s40273-021-01037-2

Lamba, S., Das, T., & Srivastava, P. K. (2024). Impact of infectious density-induced additional screening and treatment saturation on COVID-19: Modeling and cost-effective optimal control. *Infectious Disease Modelling, 9*, 569–600. https://doi.org/10.1016/j.idm.2024.03.002

Mathieu, E., Ritchie, H., Rodés-Guirao, L., Appel, C., Giattino, C., Hasell, J., Macdonald, B., Dattani, S., Beltekian, D., Ortiz-Ospina, E., & Roser, M. (2020). Coronavirus pandemic (COVID-19), our World in Data. https://ourworldindata.org/coronavirus.

Motorniak, D., Savulescu, J., & Giubilini, A. (2023). Reelin'in the years: Age and selective restriction of liberty in the COVID-19 pandemic. *Journal of bioethical inquiry*, 1–9. https://doi.org/10.1007/s11673-023-10318-8

Owusu-Dampare, F., & Bouchnita, A. (2023). Equitable bivalent booster allocation strategies against emerging SARS-CoV-2 variants in US cities with large Hispanic communities: The case of El Paso County, Texas. *Infectious Disease Modelling, 8*, 912–919. https://doi.org/10.1016/j.idm.2023.07.009

Patón, M., Acuña, J. M., & Rodríguez, J. (2023). Evaluation of vaccine rollout strategies for emerging infectious diseases: A model-based approach including protection attitudes. *Infectious Disease Modelling, 8*, 1032–1049. https://doi.org/10.1016/j.idm.2023.07.012

Perra, N. (2021). Non-pharmaceutical interventions during the COVID-19 pandemic: A review. *Physics Reports, 913*, 1–52. https://doi.org/10.1016/j.physrep.2021.02.001

Pollock, A. M., & Lancaster, J. (2020). Asymptomatic transmission of covid-19. *BMJ, 371*. https://doi.org/10.1136/bmj.m4851

Rohatgi, A. (2022). *Webplotdigitizer* Version 4.6. https://automeris.io/WebPlotDigitizer.

SAGE 56th meeting on COVID-19. https://assets.publishing.service.gov.uk/government/uploads/system/uploads/attachment_data/file/928699/S0740_Fifty-sixth_SAGE_meeting_on_Covid-19.pdf, (2020).

Sah, P., Fitzpatrick, M. C., Zimmer, C. F., Abdollahi, E., Juden-Kelly, L., Moghadas, S. M., Singer, B. H., & Galvani, A. P. (2021). Asymptomatic SARS-CoV-2 infection: A systematic review and meta-analysis. *Proceedings of the National Academy of Sciences, 118*, Article e2109229118. https://doi.org/10.1073/pnas.2109229118

Saha, A. K., Saha, S., & Podder, C. N. (2022). Effect of awareness, quarantine and vaccination as control strategies on Covid-19 with co-morbidity and re-infection. *Infectious Disease Modelling, 7*, 660–689. https://doi.org/10.2139/ssrn.4185141

Schlosser, F., Maier, B. F., Jack, O., Hinrichs, D., Zachariae, A., & Brockmann, D. (2020). COVID-19 lockdown induces disease-mitigating structural changes in mobility networks. *Proceedings of the National Academy of Sciences, 117*, 32883–32890. https://doi.org/10.1073/pnas.2012326117

Soni, A., Herbert, C., Lin, H., Yan, Y., Pretz, C., Stamegna, P., Wang, B., Orwig, T., Wright, C., Tarrant, S., et al. (2023). Performance of rapid Antigen tests to detect symptomatic and asymptomatic SARS-CoV-2 infection: A prospective cohort study. *Annals of Internal Medicine, 176*, 975–982. https://doi.org/10.7326/M23-0385

Spaccatini, F., Giovannelli, I., & Pacilli, M. G. (2022). "You are stealing our present": Younger people's ageism towards older people predicts attitude towards age-based COVID-19 restriction measures. *Journal of Social Issues, 78*, 769–789, 10.1111/josi. 12537.

Tan, W., Wong, L., Leo, Y., & Toh, M. (2020). Does incubation period of COVID-19 vary with age? A study of epidemiologically linked cases in Singapore. *Epidemiology and Infection, 148*, e197. https://doi.org/10.1017/S0950268820001995

Thongtha, A., & Modnak, C. (2022). Optimal COVID-19 epidemic strategy with vaccination control and infection prevention measures in Thailand. *Infectious Disease Modelling, 7*, 835–855. https://doi.org/10.1016/j.idm.2022.11.002

Van Rens, T., & Oswald, A. J. (2020). Age-based policy in the context of the covid-19 pandemic: How common are multigenerational households? *CAGE Online Working Paper Series*.

Vatcheva, K. P., Sifuentes, J., Oraby, T., Maldonado, J. C., Huber, T., & Villalobos, M. C. (2021). Social distancing and testing as optimal strategies against the spread of COVID-19 in the Rio Grande Valley of Texas. *Infectious Disease Modelling, 6*, 729–742. https://doi.org/10.1016/j.idm.2021.04.004

Verma, V. R., Saini, A., Gandhi, S., Dash, U., & Koya, S. F. (2020). Capacity-need gap in hospital resources for varying mitigation and containment strategies in India in the face of COVID-19 pandemic. *Infectious Disease Modelling, 5*, 608–621. https://doi.org/10.1016/j.idm.2020.08.011

Vinceti, M., Balboni, E., Rothman, K. J., Teggi, S., Bellino, S., Pezzotti, P., Ferrari, F., Orsini, N., & Filippini, T. (2022). Substantial impact of mobility restrictions on reducing COVID-19 incidence in Italy in 2020. *Journal of Travel Medicine, 29*. https://doi.org/10.1093/jtm/taac081

Wolfram Research Inc.. (2022). *Mathematica*. Version 13.1 https://www.wolfram.com/mathematica.

Wu, Y., Kang, L., Guo, Z., Liu, J., Liu, M., & Liang, W. (2022). Incubation period of COVID-19 caused by unique SARS-CoV-2 strains: A systematic review and meta-analysis. *JAMA Network Open, 5*, Article e2228008. https://doi.org/10.1001/jamanetworkopen.2022.28008

Zakary, O., Rachik, M., & Elmouki, I. (2017). A new epidemic modeling approach: Multi-regions discrete-time model with travel-blocking vicinity optimal control strategy. *Infectious Disease Modelling, 2*, 304—322. https://doi.org/10.1016/j.idm.2017.06.003

Zaman, G., Kang, Y. H., & Jung, I. H. (2009). Optimal treatment of an SIR epidemic model with time delay. *Biosystems, 98*, 43—50. https://doi.org/10.1016/j.biosystems.2009.05.006

Zhou, Y., Xu, R., Hu, D., Yue, Y., Li, Q., & Xia, J. (2020). Effects of human mobility restrictions on the spread of COVID-19 in shenzhen, China: A modelling study using mobile phone data. *The Lancet Digital Health, 2*, e417—e424. https://doi.org/10.1016/S2589-7500(20).30165-5